MASTERARBEIT | MASTER'S THESIS

Titel | Title

Improving *in vitro* Tau ubiquitination to dissect its interaction with the autophagy machinery

verfasst von | submitted by

Lara Klune BSc

angestrebter akademischer Grad | in partial fulfilment of the requirements for the degree of

Master of Science (MSc)

Wien | Vienna, 2024

Studienkennzahl lt. Studienblatt | Degree programme code as it appears on the student record sheet:	UA 066 865
Studienrichtung lt. Studienblatt | Degree programme as it appears on the student record sheet:	Masterstudium Molecular Biology
Betreut von | Supervisor:	Univ.-Prof. Dipl.-Biol. Dr. Sascha Martens Privatdoz.

Acknowledgments

First of all, I am deeply grateful to my supervisor in this project, Dr. Sascha Martens. He gave me the valuable opportunity to study my project in his lab, was always supportive and provided professional guidance when needed.

This project would not have been possible without Dr. Luca Ferrari. He provided me with my master's project and guided me all along the way. He was an inspiring, kind and patient teacher who never wavered in his friendliness and enthusiasm and gave me constant support, no matter what.

I would also like to express my heartfelt appreciation to the entire team at the Martens lab. Their valuable insights and feedback significantly enriched my work, and their camaraderie made my work experience all the more enjoyable. Their contributions were integral to the success of this project.

My sincere thanks should also go to Dr. Zuzana Hodakova, who provided significant technical expertise and generously shared lab instruments with me for a particular experiment.

I am also very grateful to Dr. David Haselbach, whose scientific expertise contributed significantly to the progress of some of my projects.

I would like to extend my thanks to the Max Perutz Labs mass spectrometry facility. I used their services several times throughout my thesis, and the analyses they provided were essential to my work.

Abstract

The ubiquitination of proteins, a highly variable and specific post-translational modification, is a crucial component of cell signaling. It plays a pivotal role in determining the fate of proteins, either by targeting them to the ubiquitin-proteasome system or autophagy, the two major degradation systems of the cell. Dysregulation of these pathways is associated with a range of diseases, including neurodegenerative conditions like Alzheimer's disease, characterized by the accumulation of abnormal Tau protein species.

In this thesis, a ubiquitination machinery composed of the E1 UBA1, an E2 (UBCH5B or UEV1:UBC13) and the E3 CHIP (+HSPA1A) was used to reconstitute the ubiquitination of the physiological substrate Tau *in vitro*. Different aspects of this process were investigated and improved, mainly concerning the specificity (in terms of length, linkage or targeted lysine residues) of the attached ubiquitin chains and their interaction with the autophagy machinery.

The EEVD motif of the molecular chaperone HSPA1A is essential for its association with the E3 ligase CHIP. A role for this motif was observed in targeting specific lysine residues of Tau for ubiquitination. Additionally, K0, K48 and K63 ubiquitin variants were employed to attempt length and linkage control of ubiquitin chains on Tau. Tau modified with specific K48- and K63-linked ubiquitin chains was tested for its affinity to autophagic cargo receptors. The p62 and NBR1 receptors displayed a surprising preference for K48-linked chains on Tau under the applied experimental settings. Lastly, this work describes several attempts at purifying ubiquitinated Tau.

Zusammenfassung

Die Ubiquitinierung von Proteinen ist ein Prozess, der die kovalente Bindung einer oder mehrerer Ubiquitin-Einheiten an spezifische Proteine umfasst. Dieser Vorgang ist ein wichtiger Schritt in vielen Signalwegen der Zelle und essentiell dafür, dass Proteine für den Abbau durch das Proteasom oder durch Autophagie markiert werden. Dies sind die beiden wichtigsten Degradierungsmechanismen der Zelle. Eine Dysregulation innerhalb dieser Signalwege und damit beim Proteinabbau kann mit diversen Krankheiten in Verbindung gebracht werden. Unter anderem mit neurodegenerative Leiden wie der Alzheimer-Krankheit, bei der es zu einer Akkumulation von abnormalen Formen des Proteins Tau kommt.

In dieser Arbeit wurden E1 (UBA1), E2 (UbcH5B oder Uev1:Ubc13) und E3 (CHIP +HSPA1A) Enzyme kombiniert, um die Ubiquitinierung von Tau *in vitro* zu rekonstituieren. Verschiedenste Aspekte der Protein-Ubiquitinierung wurden analysiert und optimiert, die vor allem die Spezifität der Ubiquitinketten (Ubiquitinketten-Länge, -Verknüpfung und Substratauswahl) betrafen.

Das EEVD Motiv von HSPA1A ist essentiell für die Verknüpfung mit der E3 Ligase CHIP. In den durchgeführten Experimenten wurde beobachtet, dass dieses Motiv, und die dadurch vermittelte Verbindung zu CHIP, eine Rolle in der spezifischen Ubiquitinierung von Tau spielen. Zusätzlich wurden K0, K48 und K63 Ubiquitin-Varianten angewandt, um spezifische Ubiquitin-Modifizierungen auf Tau herzustellen. NBR1 und p62, beides Cargo Rezeptoren der Autophagie, wurden auf ihre Affinität zu diesen spezifischen Ubiquitinketten auf Tau untersucht. Unter den angewandten experimentellen Bedingungen wurde eine überraschende Präferenz für Verknüpfungen über K48 im Vergleich zu K63 für beide Rezeptoren festgestellt. Darüber hinaus wurden verschiedene Aufreinigungsverfahren für ubiquitiniertes Tau getestet und beschrieben.

Table of Contents

Introduction

Ubiquitination is a central signaling system of the cell

Ubiquitination is arguably one of the most diverse and influential signaling systems in eukaryotes. It is performed by an enzymatic cascade of three functionally distinct components: the ubiquitin-activating enzyme (E1), the ubiquitin-conjugating enzyme (E2) and the ubiquitin-ligating enzyme (E3). This enzymatic cascade facilitates attachment of the C-terminal glycine of ubiquitin to the ε-amino group of a lysine (K) residue belonging to the substrate (Komander & Rape, 2012). This process is called monoubiquitination (Hicke, 2001), as a single ubiquitin moiety is bound to a non-ubiquitin target protein. Further ubiquitin molecules can be attached to a lysine residue on monoubiquitin via their C-terminal glycine, building ubiquitin chains. Any of the seven lysine residues of ubiquitin and the amino group of its N-terminal methionine can be used as attachment sites. Depending on which residue is used, different ubiquitin chain types are built. Chains can be linked via K6, K11, K27, K29, K33, K48, and K63 residues or via methionine at position 1 (M1). However, M1 linkages can be formed only by LUBAC (linear ubiquitin chain assembly complex), a multiprotein E3 ligase complex (Shibata & Komander, 2022). The complex was not used in this work and therefore, M1-linked chains were disregarded in this thesis. Chains can be homogeneous, meaning they possess only one linkage type. Alternatively, they can be linked heterogeneously, forming either mixed chains (different linkage types in one chain) or branched chains (where multiple lysine residues within one ubiquitin entity serve as attachment sites for chains of different linkage types). For a schematic summary of ubiquitin attachment, see Figure 1. The orientation and distance between the separate chain entities can vary for different chain types, resulting in diverse conformations. For instance, K63-linked ubiquitin chains have an open, beads on a string-like structure, while K48-linked chains possess a more compact conformation. This great structural diversity allows for the highly versatile usage of the ubiquitin code and its specific recognition by certain binding partners (Komander & Rape, 2012).

The diversity of this system already suggests that the variations in ubiquitin chain compositions might play an essential role in deciding the fate of its modified substrates. In agreement with this, several sources suggest both the length and the linkage of a ubiquitin chain to be of major importance. For instance, K48-linked ubiquitin chains were shown to be the primary signal that targets substrates for degradation via the UPS (ubiquitin proteasome system) (Finley et al., 1994). K63-linked ubiquitin chains, on the other hand, were assigned to influence mainly non-degradative processes such

as DNA repair and NF-κB signaling (Mukhopadhyay & Riezman, 2007) but also autophagy (Tan et al., 2008) – another degradation system of the cell.

The length of ubiquitin chains has also proven essential. In many cases, a minimum of four ubiquitin entities was shown to be required for effective proteasomal degradation signaling (Singh et al., 2016; Thrower et al., 2000). Additionally, the chain length of ubiquitin seems to be of great importance for the recognition by specific ubiquitin-binding proteins (Lutz et al., 2020). These examples grant significance to ubiquitin chain length and linkage as important factors in ubiquitin signaling and make chain specificity a highly relevant research subject.

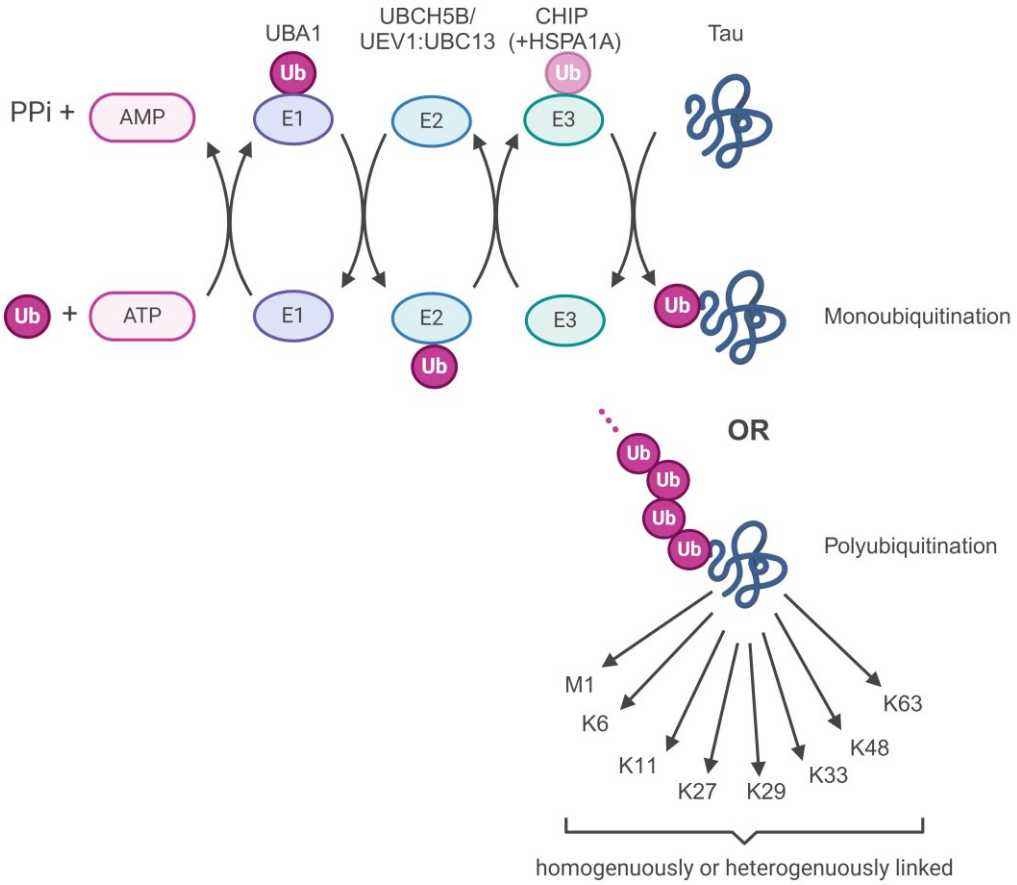

Figure 1: The mechanism of protein ubiquitination. The reaction starts in the top left corner. The E1 ubiquitin-activating enzyme uses ATP to activate and transfer ubiquitin to the ubiquitin-conjugating enzyme E2. The ubiquitin on the ubiquitin-ligating enzyme E3 is displayed in more transparent colors illustrating the possibility of ubiquitin transfer from E2 to the substrate (dark blue) without direct contact between E3 and ubiquitin. Above the symbols for the reaction constituents, the respective proteins used in this thesis are listed. The three dots above the polyubiquitinated substrate indicate that ubiquitin chains can be of variable lengths. M1, K6, K11, K27, K29, K33, K48 and K63 stand for the different linkage types found in ubiquitin chains.

Conferring specificity to ubiquitin attachment

There are four main groups of ubiquitin-ligating enzymes. RING (really interesting new gene) E3s, U-box E3s, HECT (homologous to the E6AP carboxyl terminus) E3s and RBR (RING-in-between-RING) E3s (Yang et al., 2021).

RING E3 ligases contain a RING domain. This domain binds E2 enzymes charged with ubiquitin, while another domain in the enzyme is responsible for substrate binding. The connection to substrates and charged E2s strongly enhances the transfer rate of ubiquitin to the substrate without requiring an intermediate E3-ubiquitin state (Nguyen et al., 2017; Berndsen & Wolberger, 2014). U-box E3s function similarly, but instead of a RING domain, they contain a U-box domain. While the U-box domain has a function and fold similar to that of a RING domain, it uses a network of hydrogen bonds and salt bridges instead of Zn^{2+} ion chelation to stabilize its fold (Ohi et al., 2003; Yang et al., 2021). HECT-domain ligases work via a different mechanism consisting of two distinct reactions and an intermediate E3-ubiquitin state. Substrates and Ubiquitin-charged E2s can both bind to HECT domains. The first reaction is a transfer of ubiquitin from the E2 active site cysteine to the HECT domain active site cysteine, resulting in an E3-ubiquitin state. The second reaction is the transfer of the same ubiquitin to a lysine residue on a substrate associated with the HECT ligase (Berndsen & Wolberger, 2014). Lastly, the RBR E3s can be considered RING-HECT hybrid E3 ligases. While they work via a HECT-like two-step catalytic reaction, involving an E3-ubiquitin intermediate, the reaction is enabled by the two RING domains of the ligase, one binding the charged E2 and the other containing a catalytic cysteine residue for intermediate ubiquitin attachment (Walden & Rittinger, 2018).

It is generally assumed that E3 ubiquitin ligases are the main factor responsible for substrate specificity of ubiquitin attachment (Cowan & Ciulli, 2022). Most commonly, this specificity is conferred by the recognition of a degron by the respective ligase. A degron is a short sequence located anywhere within a target protein that is vital in regulating the protein's degradation (Zheng & Shabek, 2017). However, the mechanism behind substrate recognition and binding is unclear for many E3 substrate combinations. For instance, the protein Tau (used in this thesis) has been shown to be ubiquitinated by the U-box E3 enzyme CHIP (C-terminus of HSP70 (70 kDa heat shock protein) interacting protein) (used in this work) (Petrucelli et al., 2004) but the exact way of Tau recruitment to the ligase is yet unknown. CHIP is characterized as a chaperone-dependent E3 ligase (McDonough & Patterson, 2003; T. Wang et al., 2020). Although this E3 can also work independently of a chaperone (Munari et al., 2022; Nadel et al., 2023), interactions with HSP70 family proteins like HSPA1A (heat shock protein family

A (HSP70) member 1A) (used in this thesis) were found relevant for ubiquitination of certain substrates including Tau (X. Li et al., 2008; Quintana-Gallardo et al., 2019; Shimura et al., 2004). However, even though binding sites between CHIP, HSPA1A and Tau have been characterized (Jinwal et al., 2013; Munari, et al., 2022; Sarkar et al, 2008; Scheufler et al., 2000), the function of the complex between these proteins and its formation remains poorly understood. For example, the TPR (tetratricopeptide) domain of CHIP binds the C-terminal EEVD (Glu-Glu-Val-Asp) motif of HSPA1A via a well-characterized 2-carboxylate clamp mode (Scheufler et al., 2000). The EEVD sequence is a common motif at the end of the unstructured C-terminal domains of HSP70 family proteins (Rosenzweig et al., 2019). Although this motif is known to be essential for the association between CHIP and HSP70 proteins via the abovementioned binding mode (Smith et al., 2013; Zhang et al., 2015), sources are less certain about the importance of this association for Tau recognition and ubiquitination (Munari et al., 2022; Shimura, et al., 2004). Nevertheless, an influence of HSP70 proteins on the ubiquitination of phosphorylated tau by CHIP has been previously detected (Shimura, et al., 2004). Whether HSPA1A influences Tau ubiquitination and perhaps the recognition of Tau by the E3 ligase CHIP is going to be studied more closely in this thesis.

While the responsibility for substrate specificity can be relatively clearly ascribed to E3 ligases, the production of specific chain types is thought to be determined by variable components of the ubiquitin attachment cascade. Depending on the type of E3 ligase used, E3 and E2 together or the E2 alone may determine chain linkage types (Komander & Rape, 2012). Chain specificity is believed to be conveyed by the E2 conjugating enzyme when RING or U-box domain ligases are used since they transfer ubiquitin directly from the E2 to the substrate. The E2 was proposed to mediate specificity by orienting the acceptor ubiquitin so that only specific lysine residues are exposed to the donor ubiquitin for subsequent attachment (Ye & Rape, 2009). HECT and RBR ligases, on the other hand, bind to ubiquitin themselves before ligating it to the substrate. When using these enzymes, the linkage specificity is thought to be determined by the E3 rather than the E2. The mechanism underlying linkage specificity determination by E3s is unclear (Komander & Rape, 2012). This means that the last enzyme in contact with ubiquitin most likely determines the evolving chain's linkage type.

In summary, E2 and E3 enzymes are two essential regulators enforcing the specificity of the ubiquitin code and helping to create a diverse signaling system. While this diversity allows the application of ubiquitin signaling in numerous cellular contexts, it also complicates this system's scientific resolution and understanding, as described below.

Methods to study the ubiquitin code

Research regarding the ubiquitin code and the functions it regulates has to overcome the issue of identifying the specific, complex structures ubiquitin chains can adopt in order to assign a certain signaling outcome to one particular type of modification. However, protein ubiquitination analysis remains technically challenging. Methods like MS (mass spectrometry) have been successfully applied to identify a wide range of ubiquitination sites on substrates. Additionally, simple linkage identification is possible through methods that combine, for instance, MS and specific chain enrichment techniques. However, the methodologies for identifying complex chain topologies are still scarce (Sun & Zhang, 2022). Alternative to the specific detection of various complex chain topologies, ubiquitin chains with controlled linkages can be produced *in vitro* with chemical or enzymatic methods (Y.-S. Wang et al., 2020). Enzymatic methods, which were applied in this thesis, use the E1 - E2 - E3 system to form either free ubiquitin chains or ubiquitin chains on a substrate. Specificity can, in part, be conveyed by using the correct E3 or E2 enzymes, as explained above. Enzymes with little chain specificity can be aided by employing specific ubiquitin lysine to arginine mutants that only allow certain linkages to form (Maspero & Polo, 2016; Y.-S. Wang et al., 2020).

An example can be drawn by the E2s UBCH5B and UEV1:UBC13 used in this work. When utilized in combination with CHIP+HSPA1A, they were shown to preferentially build either K27, K48 and K63 chains (UBCH5B) or K63 chains (UEV1:UBC13) (Qiu, 2021). Ubiquitin mutants allowing increased ubiquitin chain specificity in terms of length and linkage are, for instance, K48, K63 and K0 ubiquitin (used in this thesis). The names indicate the single one lysine in the protein that is not changed to arginine – so lysine at position 48, lysine at position 63 and, in the case of K0, no lysine residues remain unchanged (Figure 2). The remaining lysine residues can serve as ubiquitin attachment sites, allowing chain growth of only one linkage type. Thus, K48 ubiquitin builds only K48-linked chains, K63 ubiquitin only K63-linked chains and K0 should terminate chain growth, possibly allowing for chain length control. Therefore, UBCH5B, in combination with K48 ubiquitin, could potentially build pure K48-linked chains, and UEV1:UBC13 could build pure K63-linked chains when combined with K63 ubiquitin. Ubiquitin chains of a controlled topology could serve as a defined experimental species that might drive the resolution of the ubiquitin code.

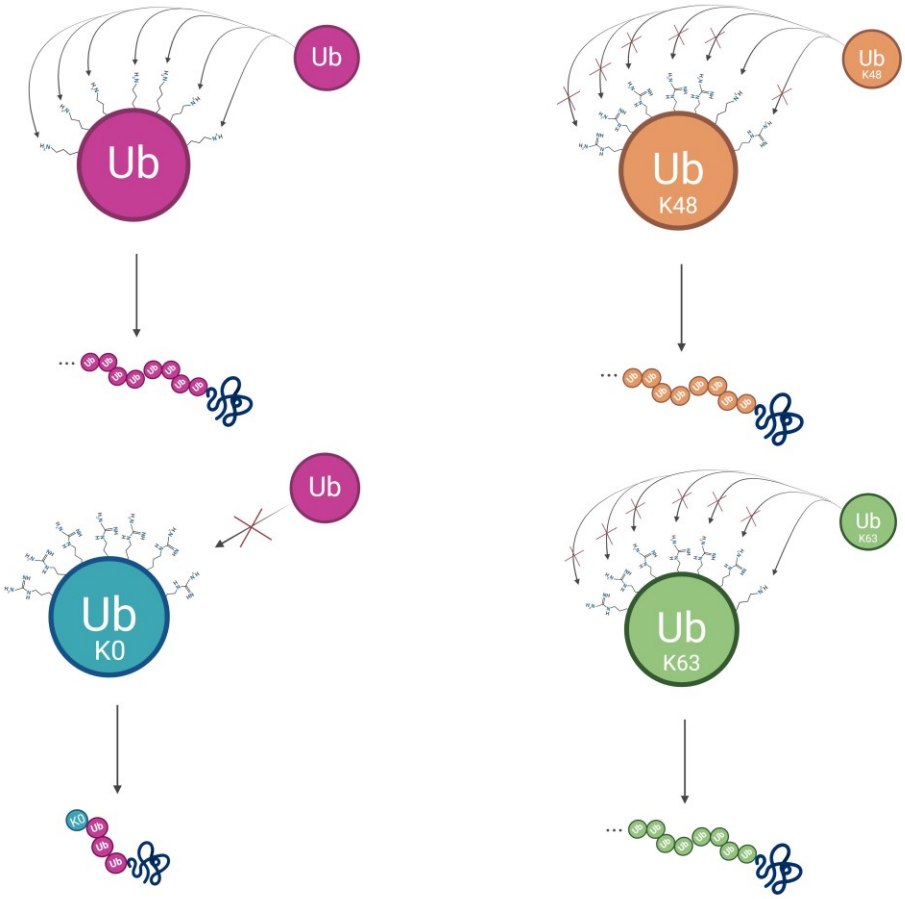

Figure 2: A depiction of the functionality of all ubiquitin mutants used in this thesis. Wild-type ubiquitin is displayed in the top left corner – each of the seven lysine residues within ubiquitin (K6 to K63 from left to right) can be used for attachment to form chains of variable lengths (illustrated by three dots next to the ubiquitin chain). The left bottom corner shows the K0 ubiquitin variant – all seven lysine residues are changed to arginine. Supplementing wild-type ubiquitin with this variant in a reaction should terminate chain extension by capping present ubiquitin chains or lysine residues in the substrate with one K0 entity. K48 (top) and K63 (bottom) ubiquitin are displayed on the right side. Both variants contain only a single lysine residue at position 48 or 63, respectively. Chains can be elongated exclusively at these lysine residues, causing chains of specific linkage types to form.

A highly relevant substrate for ubiquitination: Tau

The protein Tau is crucial to support the functional microtubule system of a cell under physiological conditions. It is associated with microtubules and plays a significant role in their assembly and stability (Medeiros et al., 2011). However, under pathological conditions, Tau can undergo hyperphosphorylation, leading to its dissociation from microtubules and accumulation in NFTs (neurofibrillary tangles) and PHFs (paired-helical filaments) and to a loss of microtubules and tubulin-associated proteins (Breijyeh & Karaman, 2020). Hyperphosphorylated Tau that is accumulated in NFTs is a central property of tauopathies (neurodegenerative diseases displaying aggregates of abnormal Tau in the brain), including AD (Alzheimer's disease) (Gendron & Petrucelli, 2009). Additionally, several sources suggest abnormal Tau to be toxic and, therefore, to be a main player causing neurodegeneration in AD (Long & Holtzman, 2019).

Abnormal Tau species can exist in various states associated with varying degrees of toxicity. The above-mentioned aggregation in NFTs and PHFs is proposed to be less toxic than its precursor: soluble, oligomeric Tau. Soluble Tau oligomers are considered the most neurotoxic Tau species (Ghag et al., 2018). An influence of ubiquitination on the distribution of Tau into those different states was suggested. For instance, Dickey et al. (2006) show that CHIP – an E3 well known for Tau ubiquitination – polyubiquitinates Tau, enhances the formation of insoluble filaments, as compared to soluble oligomers, and mediates Tau degradation. Subsequently, L. Li et al. (2022) hypothesize that polyubiquitination of Tau oligomers might lead to insoluble Tau formation and its subsequent degradation, assigning a protective role to ubiquitination against the toxicity of soluble Tau oligomers.

This protective role could be explained by ubiquitin's function in the degradation of abnormal or aggregated proteins. As mentioned above, K48- and K63-linked ubiquitin chains are strongly linked to the UPS and autophagy, respectively (Finley et al., 1994; Tan et al., 2008). The identification of both linkage types in an AD context supports the idea that ubiquitination might matter for abnormal Tau reduction in disease. For instance, K48-linked ubiquitin chains were found in PHFs (Morishima-Kawashima et al., 1993), and K63-linked ubiquitin attached to soluble Tau oligomers could be detected at heightened levels in AD brains (Arakhamia et al., 2020; Puangmalai et al., 2022; Wesseling et al., 2020).

Taken together, this grants great significance to ubiquitinated Tau as a protein species closely associated with AD and the cell's two major degradation systems (Lee et al., 2013). Therefore, it is a very attractive substrate to study, especially in an AD-, autophagy- or UPS-related context.

Maintaining homeostasis via protein degradation

Autophagy and the UPS are the two main degradation systems of the cell and are essential for the maintenance of cellular homeostasis. Amongst a vast number of targets, also Tau is indicated to be targeted by both pathways (Lee et al., 2013). While the UPS is believed to target mainly soluble misfolded proteins and short-lived proteins, autophagy is thought to degrade preferentially long-lived proteins and large structures like protein aggregates and organelles (Kocaturk & Gozuacik, 2018). Nevertheless, autophagy was also proposed to degrade endogenous Tau when activated as a compensatory response to an inhibition of the proteasome (Krüger et al., 2012). Both pathways have in common the ability to recognize targets based on their modification by ubiquitin (Kocaturk & Gozuacik, 2018).

In this thesis, the term autophagy is used synonymously with macro-autophagy. In autophagy, cargo destined to be degraded, such as organelles or protein aggregates, are engulfed by a growing phagophore (also known as isolation membrane), forming a double-membrane-autophagosome upon closure. The autophagosome is then transported to the lysosome, where its outer membrane fuses with the lysosomal membrane. The inner membrane enclosing the cargo is released into the acidic environment of the lysosome, where degradation is initiated (Adriaenssens et al., 2022; Glick et al., 2010).

Compared to starvation-induced bulk autophagy, cargo can be specifically recognized by so-called cargo receptors in selective autophagy. A specific form of selective autophagy is specialized in the degradation of aggregated proteins – it is termed aggrephagy. Tau aggregates might form a cargo for this very pathway. p62 (also known as SQSTM1) and NBR1 are well-studied cargo receptors in aggrephagy (Adriaenssens et al., 2022; Bauer et al., 2023). They can recognize ubiquitinated substrates via their UBA (ubiquitin-associated) domains. p62 was shown to be particularly attracted by K63-linked ubiquitin chains, aligning with the common opinion that this is the primary linkage type signaling to the autophagy machinery (Tan et al., 2008; Wurzer et al., 2015). The p62 and NBR1 cargo receptors can hetero-oligomerize using their PB1 domains. p62, in contrast to NBR1, can also oligomerize with itself (Ciuffa et al., 2015; Lamark et al., 2003). These interactions via, on the one hand, the cargo receptor's own PB1 domains and, on the other hand, with ubiquitin, promote the sequestration of ubiquitinated proteins into larger condensates. In turn, other factors can be recruited, finally inducing the biogenesis of autophagosomes at the cargo site (Bauer et al., 2023; Turco et al., 2021). The growing phagophore membrane contains ATG8 family proteins, which can be bound by the LIR (LC3-interacting) motifs within p62 and NBR1, tethering the cargo to the autophagic membrane until its biogenesis is completed (Adriaenssens et

al., 2022; Bauer et al., 2023). The process of aggrephagy is explained schematically in Figure 3.

Instead of using the lysosome of a cell, the UPS uses a large protein complex specialized in unfolding and breaking apart proteins for degradation. This complex is called the 26S proteasome. It is composed of a core particle (20S proteasome) and two regulatory particles (19S complexes), which form cap-like structures on either end of the core particle (Figure 3). While the core is responsible for proteolysis, the regulatory particles hold multiple functions, such as polyubiquitin chain recognition and removal, and also target protein entrapment, unfolding and subsequent transfer into the core particle. As implied before, the recognition of proteins destined for degradation by the 26S proteasome depends on the previous attachment of ubiquitin chains to the targets (Groll & Huber, 2003; Tanaka, 2009).

As discussed before, the diversity and specificity of ubiquitin chains are suggested to play major roles in deciding whether a protein will be degraded by autophagy or by the UPS. However, the details of this decision process remain unclear, not least due to the technical difficulties in generating defined ubiquitinated species of a substrate of interest.

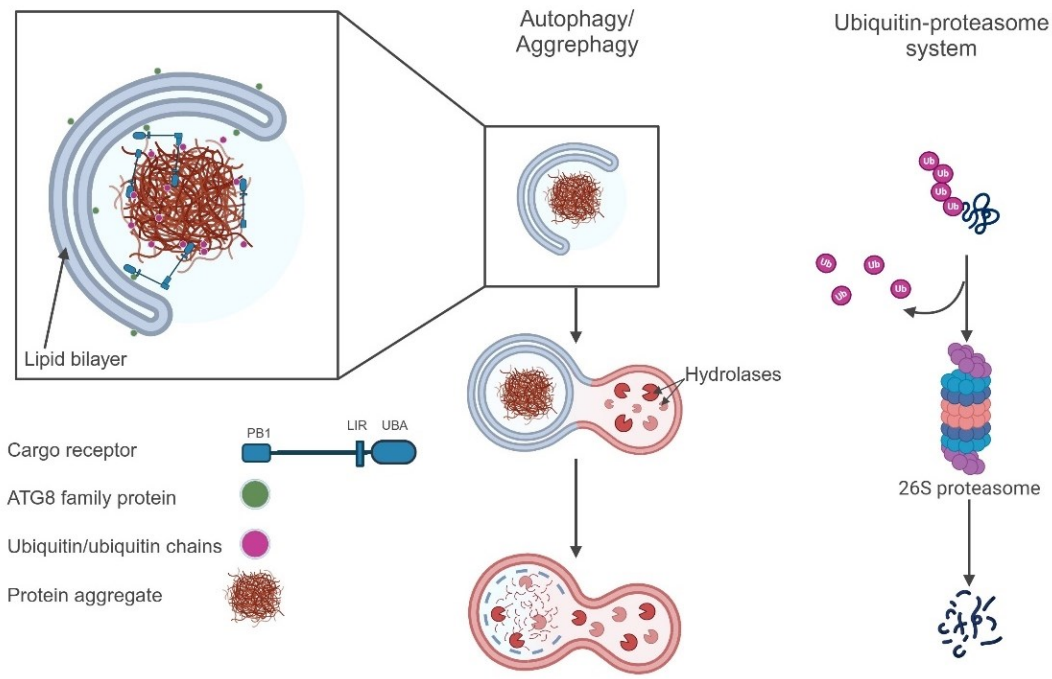

Figure 3: A schematic diagram explaining autophagy, or, more specifically, aggrephagy, and the UPS. On the left, a zoom-in of phagophore expansion is shown. The single components of the zoom-in are listed below. The cargo receptor shown here is structurally based on p62 but is representative of any cargo receptor used during aggrephagy. Although p62 can form larger complexes (Ciuffa et al., 2015), only dimers are shown for the sake of simplicity. In the middle of the diagram, aggrephagy is depicted, and degradation via the UPS is displayed on the right.

In this thesis, an enzymatic *in vitro* ubiquitination assay was used to investigate several aspects concerning the ubiquitination of Tau and its interaction with the autophagy machinery. This includes mainly the specificity of ubiquitin chains on Tau in terms of length, linkage and targeted lysin residues. The ubiquitination assay utilizes a combination of E1 (UBA1), E2 (UEV1:UBC13 or UBCH5B) and E3 (CHIP + HSPA1A) to covalently attach ubiquitin to the physiological substrate Tau (isoform 2N4R). A possible role for HSPA1A's association with CHIP, via the EEVD-TPR interaction, in the ubiquitination of specific sites on Tau was discovered. Additionally, specifically K48- and K63-linked ubiquitin chains on Tau were built with the aid of the K48 and K63 ubiquitin variants. Ubiquitin chain length control was attempted by employing the K0 ubiquitin variant. The affinity of p62 and NBR1 autophagy cargo receptors for specific K48- versus K63-linked ubiquitin chains on Tau (using K48 and K63 ubiquitin) was investigated. Both cargo receptors, surprisingly, showed stronger binding to K48-linked chains under the applied experimental settings, contrary to the idea that the primary signal for autophagy is K63-linked ubiquitin chains. Lastly, several approaches for the complete purification of ubiquitinated Tau were tested.

Materials and Methods

Antibodies

Table 1: The antibodies used for Western blots or bead-based purifications.

Antibody	Source
Mouse anti-FLAG 6B2	Ogris Lab
Mouse anti-Ubiquitin (FK2/UBCJ2)	Enzo
Goat anti-Mouse IgG HRP	Dianova

Plasmids

Table 2: The plasmids used for or produced by cloning.

Plasmid	Construct code
pRK5-HA-Ubiquitin-K0	SMc1826
pRK5-HA-Ubiquitin-K48	SMc1827
pRK-HA-Ubiquitin-K63	SMc1828
pET-Ubiquitin-K0	SMc1853
pET-Ubiquitin-K48	SMc1854
pET-Ubiquitin-K63	SMc1855
pET-HSPA1A	SMc1473
pET-HSPA1A-dEEVD	SMc1857
pGEX-TUBE	SMc1856
pET-Duet1	SMc67
pGEX-4T1	SMc49

SDS-PAGE (sodium dodecyl sulfate-polyacrylamide gel electrophoresis)

The samples for SDS-PAGE were prepared by adding 5x PLD (protein loading dye; 313 mM Tris-Cl pH 6.8, 50% glycerol, 10% SDS, 0.5% Bromphenol-Blue sod salt) to the protein sample and boiling the mixtures for 5-10 minutes at 95°C. A protein marker (PageRuler Prestained Protein Ladder, Thermo Scientific) was loaded next to the samples for protein size determination.

For protein purification samples, 12 or 15% polyacrylamide gels were used together with SDS running buffer diluted from 10x stock (250 mM Tris, 1.9 M glycine, 1% SDS). For all assays, commercial Bolt 4-12% Bis-Tris Plus gradient gels (Invitrogen) were used together with MES SDS running buffer diluted from 20x stock (1 M MES, 1 M Tris, 16 mM EDTA, 2% SDS). All gels were run at 250 volts for about 25 minutes or until the dye reached the bottom.

Coomassie staining

Gels were stained for 5-10 minutes in Coomassie Brilliant Blue stain (0.06% Coomassie Brilliant Blue in destaining solution) and destained in destaining solution (40% EtOH, 10% Acetic Acid) for roughly 20 minutes. The gels were destained entirely in dH_2O (distilled water) overnight. If the gels were further analyzed by mass spectrometry, they were kept in dH_2O at 4°C for up to 2 weeks until the analysis.

Western blot

For the identification of a particular protein - in this case, FLAG Tau - a Western blot analysis was conducted. Protein bands were transferred from the precast gradient gels mentioned above to a PVDF 0.2 µm transfer membrane (Thermo Scientific) previously activated in methanol for 2 minutes. The transfer was done in a Bio-Rad chamber for 17 hours with 30 milliamperes. After the transfer, the membrane was blocked in TBS-3% milk for 1 hour (all incubation steps were performed at room temperature, shaking gently). Next, the membrane was incubated for 1 hour with the primary anti-FLAG antibody diluted 1:200 in TBST-3% milk (always 0.1% TWEEN 20, Sigma-Aldrich). The membrane was washed with TBST three times for 10 minutes each. The secondary Goat anti-Mouse antibody was diluted 1:10000 in TBST-3% milk and incubated with the membrane for 45 minutes. The membrane was rewashed thrice for 10 minutes each. The membrane was imaged with a ChemiDoc MP Imaging System (Bio-Rad) directly after 1-5 minutes of incubation in a 1:1 mixture of Clarity Western ECL Substrate (Bio-Rad).

Mass spectrometry

Mass spectrometry was applied to identify and characterize the ubiquitination on the substrate FLAG Tau. For that, the bands of interest were cut from a precast gel, which was run as explained above. The Max Perutz Labs Mass Spectrometry Facility then analyzed the samples.

Band intensity quantification

The intensity of bands on either a Coomassie gel or a Western blot was determined using the ImageJ plugin _BandPeakQuantification.ijm (https://www.protocols.io/view/quantification-of-gel-bands-by-an-image-j-macro-ba-7vghn3w?step=8).
The gel or blot of interest was opened in FIJI, and the color was inverted by clicking "Invert" in the "Edit" tab. By clicking "Tools" and then "ROI Manager" in the "Analyze" tab, the ROI (region of interest) Manager was opened. With the "Rectangle" or "Oval" selection tool, the ROIs were selected and added to the ROI Manager by pressing "Ctrl + T". The previously installed plugin was selected, and the program was started by employing the following settings:
background width: 3
estimate background from: all
background estimation by: median.
The program produces several outputs. The one of importance is labeled "Signal". It gives the background-corrected integrated intensity and is used as the intensity value for further analysis.

Display of results

SDS gels and Western blots were annotated using GIMP.
Schemes were designed, and highlights were added to gels or blots using BioRender.
Graphs were created with Microsoft Excel.
Bead experiments were analyzed using a script available in the lab.

Cloning

For the K0 (all lysine residues mutated to arginine), K48 (all lysine residues except for residue 48 changed to arginine) and K63 (all lysine residues except for residue 63 changed to arginine) ubiquitin variants, the coding sequences of the respective plasmids were purchased from Addgene and subcloned into empty pET-Duet1 vectors suitable for bacterial expression.

For that, the coding sequences from the Plasmids pRK5-HA-Ubiquitin-K0 (Addgene ID: #17603), -K48 (Addgene ID: #17605) and -K63 (Addgene ID: #17606) were amplified by a PCR (polymerase chain reaction) using primers that would allow insertion into the empty pET-Duet1 vector directly downstream of the Histidine tag sequence via restriction enzyme cloning. Primers were ordered from Microsynth. The PCR was performed using Q5 High-Fidelity DNA Polymerase (BioLabs) and Q5 Reaction Buffer (BioLabs) with the recommended reaction times for the specific polymerase. The reactions were carried out in a T100 Thermal Cycler (Bio-Rad). The melting temperature was calculated using the NEB Tm Calculator. The success of the PCR was checked by loading 5 µl of the reaction plus 1 µl Gel Loading Dye, Purple (6x) (BioLabs) on a 1% agarose gel next to a marker (GeneRuler 1 kb Plus, Thermo Scientific) and then visualizing it under blue light. The PCR product was cleaned with the ReliaPrep DNA Clean-Up and Concentration System (Promega). The DNA was then cleaved for 30 minutes at 37°C with the enzymes Not1 HF (BioLabs) and BamH1 HF (BioLabs) in the presence of CutSmart Buffer (BioLabs). The product was mixed with the correct amount of 6x loading dye and run on a 1% agarose gel. After checking under blue light, the correct bands were cut out from the gel and cleaned up, and then the concentration was determined with a nanodrop spectrophotometer (DeNovix). The amplified insert was added to a ligation reaction with the empty vector in a 1:1 ratio. The reaction was performed with T4 DNA Ligase (BioLabs) and T4 DNA Ligase Reaction Buffer (BioLabs) for 16 hours at 16°C. The remaining linear DNA was digested with Plasmid-Safe ATP-dependent DNase (Lucigen), Plasmid-Safe 10x Reaction Buffer (Lucigen) and ATP Solution (Lucigen) for 30 minutes at 37°C, followed by a 30-minute incubation at 70°C. The DNA was then transformed into DH5α Competent Cells (ThermoScientific) via heat shock. The cells were grown on 2xTY plates with ampicillin overnight. 4 ml of LB medium plus ampicillin were inoculated, each with one colony from the plates, and incubated overnight, shaking at 37°C. The cultures were spun down for 15 minutes at 4°C and 3220 g, and the supernatant was discarded. The plasmids were isolated from the cell pellet with the GeneJET Plasmid Miniprep Kit (ThemoScientific). 10 µl of each plasmid were cleaved in the same manner as above, and the products were again checked on an

agarose gel. Once the correct bands for the plasmid and inserts could be detected, the clean plasmids were sent for sequencing to Microsynth using primers covering the whole insert.

The EEVD motif deletion variant of HSPA1A (HSPA1A dEEVD) was subcloned from a pET-HSPA1A construct available in the lab (SMc1473). When the insert sequence was amplified, the reverse primer was designed in a way that the stop codon would come before the EEVD motif, excluding it from the PCR. The cleavage steps were performed with Not1 HF (BioLabs) and EcoR1 HF (BioLabs). Otherwise, the cloning was performed as described above.

The TUBEs (tandem ubiquitin-binding entities) construct was subcloned from a mammalian expression vector containing the FLAG TR-TUBE (trypsin-resistant-TUBE), which the Fumiyo Ikeda lab kindly provided. After amplifying the insert sequence, not including the FLAG sequence, it was inserted into an empty pGEX-4T1 plasmid via Not1 and BamH1 restriction sites. Apart from that, the cloning was performed as for the ubiquitin variants.

Protein expression and purification

The various pET-Ubiquitin constructs were expressed in 2xTY medium with ampicillin after their heat shock transformation into Rosetta (DE3) Competent Cells (Novagen). The expression was performed overnight at 18°C in the presence of 0.15 mM IPTG (Isopropyl-ß-D-thiogalactopyranosid - Sigma-Aldrich). The harvested cell pellets were first resuspended and frozen in lysis buffer (25 mM HEPES, 150 mM NaCl, 25 mM Imidazole, 2 mM ß-Mercaptoethanol, protease inhibitor tablet - Roche EDTA free) and then lysed by sonication (3 times with 30-second treatments, five cycles, 60-65% power) with a sonicator (Bandelin) after adding a pinch of DNase. The cell lysate was cleared by centrifugation for 60 minutes at 200000 g (rotor: Ti45) and 4°C. The supernatant was filtered through a 0.45 µm filter with a syringe. Purification was performed using a 5 ml HisTrap HP column (Cytiva) equilibrated in HisTrap buffer A (25 mM HEPES, 150 mM NaCl, 25 mM Imidazole, 2 mM ß-Mercaptoethanol). The sample was eluted with a step gradient of buffer B (25 mM HEPES, 150 mM NaCl, 400 mM Imidazole, 2 mM ß-Mercaptoethanol) from 0% (25 mM Imidazole) up to 100% (400 mM Imidazole). The protein eluted at the 50% step. The Histidine tag was removed during an overnight incubation of the sample at 18°C with 50 µl of TEV (tobacco etch virus) protease. The sample was then concentrated with an Amicon concentrator 3 kDa MWCO (Millipore) and spun

down for 10 minutes at 16000 g and 4°C before it was loaded onto a HiLoad 16/600 Superdex 75 pg size exclusion column (Cytiva) equilibrated with SEC buffer (25 mM HEPES, 150 mM NaCl, 1 mM DTT). The pure protein was concentrated, aliquoted, and snap-frozen in liquid nitrogen. After thawing, concentration measurements were performed at a nanodrop spectrophotometer using the absorbance at 280 nm and the extinction coefficient calculated with the ProtParam algorithm at ExPasy (https://web.expasy.org/protparam/).

TUBEs were expressed, harvested and lysed as described above but with a different lysis buffer (50 mM Sodium Phosphate, 300 mM NaCl, 2 mM ß-Mercaptoethanol, protease inhibitor tablet - Roche EDTA free). The lysate was cleared by centrifugation for 15 minutes at 200000 g (rotor: Ti45) and 4°C. The supernatant was filtered with a 0.2 µm filter. The Purification was performed using a GST (Glutathione S-transferase) resin (Glutathione Sepharose, Cytiva) equilibrated with wash buffer (50 mM HEPES, 300 mM NaCl, 1 mM DTT). The beads were incubated with the supernatant for 1 hour at 4°C, rolling. After washing the beads five times, the elution was performed with 10 ml elution buffer (50 mM HEPES, 300 mM NaCl, 20 mM L-Glutathione, 1 mM DTT) for 1 hour at room temperature. Again, the supernatant was filtered with a 0.2 µm filter and then concentrated with an Amicon concentrator 30 kDa MWCO (Millipore). After spinning the sample down for 10 minutes at 16000 g and 4°C, it was loaded onto a Superdex 200 Increase 10/300 GL size exclusion column (Cytiva) equilibrated in SEC buffer. Concentration measurement and storage were performed as above.

The dEEVD variant was expressed similarly to the ubiquitin variants but with 0.12 mM IPTG. Harvest and lysis were performed identically to the ubiquitin mutants. Lysate clearance was performed at 4°C and 200000 g (rotor: Ti45) for 45 minutes. After filtering the supernatant (0.45 µm), it was loaded onto a 5 ml HisTrap HP column (Cytiva) equilibrated with HisTrap buffer A. The wash step after loading was stopped after 2.5 CV (column volumes). A manual wash step with 5 CV of high salt buffer (25 mM HEPES, 1 M NaCl, 2 mM ß-Mercaptoethanol) was performed, followed by a manual wash with 2 CV of ATP buffer (25 mM HEPES, 150 mM NaCl, 5 mM $MgCl_2$, 1 mM ATP, 2 mM ß-Mercaptoethanol). The ATP buffer wash step removes unwanted HSP70 substrates associated with the chaperone by decreasing the chaperone's substrate affinity. The column was closed and put for incubation at 4°C, rolling for 30 minutes. Subsequently, the column was reconnected with the system, and the elution was performed as described above. Peaks from 15 and 25% were collected to continue with an overnight TEV cleavage (50 µl TEV protease at 4°C, rolling). After the

cleavage, the sample was concentrated using an Amicon concentrator 30 kDa MWCO (Millipore) and then spun down for 10 minutes at 16000 g and 4°C. The supernatant was loaded onto a HiLoad 16/600 Superdex 200 pg column equilibrated with SEC buffer. Storage and concentration measurements were performed as stated above.

Luca Ferrari purified FLAG Tau (isoform 2N4R). Additionally, a slightly simpler version of the same purification was attempted and is described in the following paragraph. An SDS gel comparing the products from the two different purification strategies can be seen in Figure 4. The ion exchange step in the original purification protocol was omitted in the simplified version. The result was slightly less pure Tau as a product. The purification was similar to the one described for the ubiquitin variants but with minor variations: the lysate was cleared by centrifugation at 150000 g (rotor: Ti45) and 4°C for 1 hour. The size exclusion was performed with a HiLoad 16/600 Superdex 200 pg column equilibrated in SEC buffer. The Bradford method was used for protein concentration measurements.

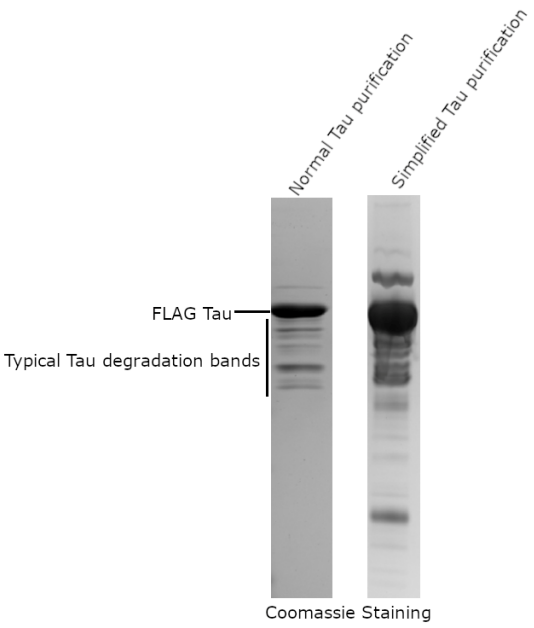

Figure 4: A Coomassie-stained SDS gel of the Tau from Luca Ferrari's purification (Normal Tau purification) and my simplified FLAG Tau purification. Tau remained the most prominent band also after the simplified purification and displayed the typical degradation bands always seen for this protein. Apart from that, several faint bands could be seen above and below the typical Tau bands. Those, most likely, represented slight impurities that were not present after the standard purification protocol.

After each purification column (of every purification), the resulting fractions were checked by SDS-PAGE and Coomassie staining to choose the correct fractions for the following purification steps or the final protein sample. SDS gels also served to determine the purity of the final protein.
All buffers that were used with a purification column were filtered and degassed.
Other proteins that were used in the experiments were provided by members of the lab.

Ubiquitination of FLAG Tau

Table 3: The reagents for a ubiquitination reaction mix in the order of addition. Protein variants were used interchangeably depending on the type of experiment following the ubiquitination. wt stands for the wild-type version of the protein.

Ingredients	Final concentrations
dH_2O	-
Ubiquitination Buffer 10x	1x
UBA1	50 nM
Ubiquitin (wt/K48/K63/K0)	10 µM
FLAG Tau (normal/less pure)	1.5 µM
HSPA1A (wt/dEEVD)	1 µM
CHIP	2.5 µM
UEV1:UBC13/UBCH5B	5 µM
ATP	5 mM

Ubiquitination buffer (250 mM Tris HCl pH 7.5, 1200 mM NaCl, 10 mM $MgCl_2$) was previously prepared and then frozen as aliquots at -20°C for storage.
For the ubiquitination of FLAG Tau, all required proteins (Table 3) were thawed on hand and immediately spun down for 10 minutes at 4°C and 16000 g. After thawing, the proteins were kept on ice. DTT was added to the 10x ubiquitination buffer to reach a concentration of 3 mM. The reagents of the reaction mix were added on ice, and only after ATP addition, the reaction was started at 30°C. Reaction times varied depending on the subsequent experiment.
Depending on the experiment, SDS samples were taken at specific time points throughout the ubiquitination reaction. 8 µl of sample were mixed with 2 µl of 5x PLD. Figure 5 shows an example gel of a ubiquitination reaction.

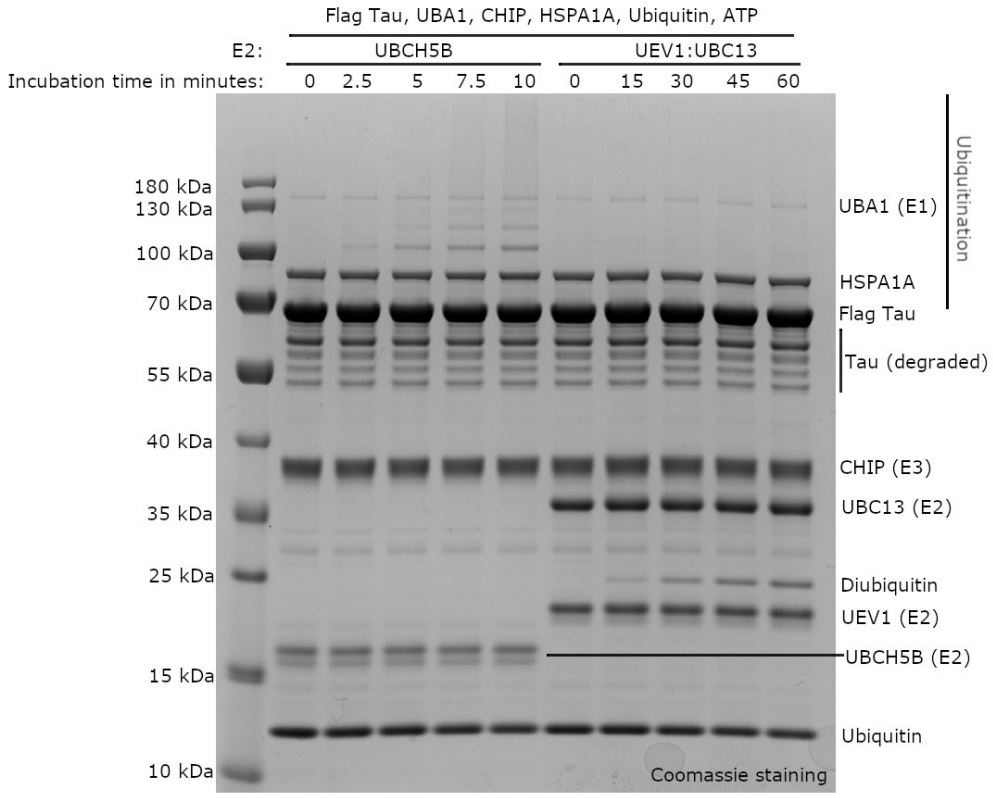

Figure 5: An image of a Coomassie gel of ubiquitination reactions with the two different E2 enzymes used throughout the experiments in this thesis. This is an example gel showing all the protein components of the reaction and their molecular weight on an SDS gel. Although most proteins run higher than their actual molecular weight, the gel matches the proteins' running behavior previously observed in our lab. Samples were taken at different time points to show the progressing ubiquitination. Ubiquitin wt and HSPA1A wt were used. The unlabeled bands and smear that can be seen in the region labeled as 'Ubiquitination' result from ubiquitin attachment to a substrate (Tau, amongst others).

Purification of ubiquitinated Tau via Dynabeads and UBCJ2/FK2 antibody

A ubiquitination reaction was performed, as explained above. For this experiment, the reaction was performed with the less pure version of Tau, the ubiquitin wt, the HSPA1A wt and UEV1:UBC13. After 1 hour reaction time, an SDS sample was taken, and the residual reaction was added to Dynabeads Protein G for Immunoprecipitation (Invitrogen) following the official protocol for Immunoprecipitation using Protein G - 10003D. The crosslinking step was omitted, and a gentle, non-denaturing elution was performed. The protein was eluted with the recommended buffer (Glycine buffer) as well as with a range of other buffers (Table 4). After an acidic elution, the pH of the eluate was adjusted, as reported in Table 5. If the sample was diluted in a high volume after adjustment (e.g., 400 µl), it was concentrated with an Amicon concentrator 3 kDa MWCO to a volume comparable in protein concentration to the other samples.

Table 4: The elution buffers that were used to elute the protein of interest from the Dynabeads.

Elution buffer	Ingredients	Elution conditions
Glycine buffer	50 mM glycine, pH adjusted 2.8, 0.2 µm filtered	2 minutes, room temperature, rolling
Citrate buffer	9.38 mM Sodium Citrate dihydrate, 90.62 mM citric acid, pH adjusted 3	2 minutes, room temperature, rolling
$MgCl_2$	3.5 M $MgCl_2$, pH measured 4.5	30 minutes, room temperature, rolling
Arginine	0.91 M arginine, pH adjusted 4.25	30 minutes, room temperature, rolling
Sarkosyl buffer	50 mM Tris pH 8, 140 mM NaCl, 1 mM EDTA, 0.3% sarkosyl, 1% glycerol, 0.2 µm filtered	20 minutes, 37°C, rolling
GST 4x ubiquitin	SEC buffer + 50, 150, 250 or 300 µM GST 4x ubiquitin	1 hour, room temperature, rolling
Free K63 ubiquitin chains	SEC buffer + 100, 250 or 500 µM free K63 ubiquitin chains	1 hour, room temperature, rolling

Table 5: The different strategies and reagents that were used to adjust the pH after elution from the Dynabeads.

Elution buffer	Adjustment with	Adjustment strategy
Glycine buffer	1 M Tris pH 7.5	Add Tris until pH 7.5
Glycine buffer	1 M HEPES pH 7.5, 5 M NaCl, 1 M DTT	Add HEPES until pH 7.5, DTT to 1 mM, NaCl to 150 mM
Glycine buffer	1 M HEPES pH 7.5, 5 M NaCl, glycerol, 1 M DTT	Add glycerol to 10%, NaCl to 300 mM, DTT to 1 mM, HEPES until pH 7.5
Glycine buffer	1 M HEPES pH 7.5, 5 M NaCl, 1% CHAPS, 1 M DTT	Add CHAPS to 0.1%, NaCl to 150 mM, DTT to 1 mM, HEPES until pH 7.5
Glycine buffer	SEC buffer	Add 400 µl SEC buffer
Glycine buffer	1 M Tris pH 8.5	Add Tris until pH 8.5
Glycine buffer	1 M MES pH 6.5	Add MES until pH 6.5
Glycine buffer	1 M MES pH 5.5	Add MES until pH 5.5

Glycine buffer	Mixed: 25 mM Tris pH 8.5, 500 mM NaCl	Add 400 µl of the mix or dialyze overnight
Glycine buffer	Mixed: 25 mM MES pH 6.5, 500 mM NaCl	Add 400 µl of the mix or dialyze overnight
Glycine buffer	Mixed: 25 mM MES pH 5.5, 500 mM NaCl	Add 400 µl of the mix or dialyze overnight
Glycine buffer	Mixed: 25 mM Tris pH 8.5, 50 mM L-Arg, 50 mM L-Glu	Add 400 µl of the mix or dialyze overnight
Glycine buffer	Mixed: 25 mM MES pH 6.5, 50 mM L-Arg, 50 mM L-Glu	Add 400 µl of the mix or dialyze overnight
Glycine buffer	Mixed: 25 mM MES pH 5.5, 50 mM L-Arg, 50 mM L-Glu	Add 400 µl of the mix or dialyze overnight
Glycine buffer	Mixed: 25 mM Tris pH 8.5, 500 mM NaCl, 50 mM L-Arg, 50 mM L-Glu	Add 400 µl of the mix or dialyze overnight
Glycine buffer	Mixed: 25 mM MES pH 6.5, 500 mM NaCl, 50 mM L-Arg, 50 mM L-Glu	Add 400 µl of the mix or dialyze overnight
Glycine buffer	Mixed: 25 mM MES pH 5.5, 500 mM NaCl, 50 mM L-Arg, 50 mM L-Glu	Add 400 µl of the mix or dialyze overnight
Glycine buffer	Citrate buffer	Buffer exchange (three centrifugation cycles, 16000 g, Amicon concentrator 3 kDa MWCO, in total 1:1000 dilution), then add 400 µl SEC buffer
Citrate buffer	SEC buffer	Add 400 µl SEC buffer
$MgCl_2$	SEC buffer	Add 400 µl SEC buffer
Arginine	SEC buffer	Add 400 µl SEC buffer

Purification of ubiquitinated Tau via TUBEs

A ubiquitination reaction was performed with the less pure version of Tau, the ubiquitin wt, the HSPA1A wt and UEV1:UBC13. The reaction was carried out for 2 hours, and afterward, the reaction tubes were kept on ice until they were used. Meanwhile, Glutathione Sepharose (Cytiva) was prepared by washing twice: first, with a tenfold volume of water and second, with a tenfold volume of wash buffer (50 mM HEPES, 300 mM NaCl, 1 mM DTT). The wash steps were performed by adding the respective washing solution in a way that ensures the resuspension of all beads. This was followed by a 2-minute centrifugation step at 3000 g - with the slow breaking setting activated - and the removal of the supernatant (the washing procedure and centrifugation settings remained unchanged throughout the assay). After the washes, 0.25 mg of TUBEs were added to 10 µl of beads and incubated for 1 hour at 4°C, rolling. Subsequently, the beads were washed three times with wash buffer and transferred entirely to the ubiquitination reaction performed beforehand. After incubating this for 1 hour at room temperature while rolling, the beads were spun down, and the supernatant was discarded. Three washes were performed with wash buffer, and then the beads were split into four equal fractions, which were treated with four different elution buffers (Table 6).

Table 6: The different strategies used to elute the protein of interest from TUBEs.

Elution buffer	Elution conditions	Elution time
Free K63 ubiquitin chains, 600 µM	Rolling at room temperature	16 hours
GST 4x ubiquitin, 600 µM	Rolling at room temperature	16 hours
$MgCl_2$	Rolling at room temperature	16 hours
Glycine buffer	Rolling at room temperature	2 minutes

Purification of ubiquitinated Tau via M2 anti-FLAG beads

After isolating all ubiquitinated proteins, the second step for the purification of ubiquitinated Tau was selecting for FLAG Tau, thereby ending up with pure ubiquitinated Tau. For this, it was assumed that only 5% of the Tau used in the ubiquitination reaction was ubiquitinated (as determined by band intensity quantification previously performed in the lab) and that no losses occurred during the first purification step. A corresponding amount of Anti-FLAG M2 affinity Gel A2220 (Thermo Fisher) was used, considering that 10 µl of beads would be saturated with 6 µg of protein. The beads were cleaned with roughly a hundredfold volume of SEC buffer, vortexing for 5 seconds and spinning down at 4°C and 7000 g for 60 seconds (mixing and centrifugation settings remained unchanged throughout the assay). The ubiquitinated proteins plus 1 mM ATP were added to the cleaned beads (ATP is added throughout this protocol to open the conformation of HSPA1A so it can release its substrate Tau). This mixture was then incubated for 1 hour at 4°C, rolling. The incubation was followed by centrifugation and removal of the supernatant. The beads were then washed for 1 hour at 4°C, rolling, this time with SEC buffer plus 5 mM ATP plus 5 mM $MgCl_2$. The mixture was spun down again and washed once with SEC buffer plus 1 mM ATP and twice with standard SEC buffer. To the clean beads loaded with FLAG Tau, FLAG-peptide (Thermo Fisher) was added in a 2:1 molar ratio at a 400 ng/µl concentration. This was incubated for 1 hour at room temperature, gently rolling. After spinning down, the supernatant was transferred to a dialysis tube. 10 cm of 3.5 kDa dialysis membrane (Spectra standard RC tubing) were used, and the dialysis was performed with a thousandfold volume of SEC buffer overnight at 4°C. The next day, the dialyzed protein was transferred to an Amicon concentrator 3 kDa MWCO (Millipore) and concentrated at 16000 g and 4°C to roughly 1/10 of the initial volume. After taking an SDS sample, the final protein was aliquoted, snap-frozen in liquid nitrogen and stored at -80°C.

K0 ubiquitin titration

In this assay, the different ubiquitin mutants were used in varying ratios to ubiquitinate Tau. For this, a ubiquitination reaction was performed, as explained above, with some modifications concerning the usage of E2s and ubiquitin. In this experiment, the relative amount of K48 or K63 ubiquitin varies relative to the amount of K0 ubiquitin. Depending on the usage of either K48 or K63 mutant, UBCH5B or UEV1:UBC13 were applied, respectively.
In total, 10 ubiquitination reactions were started. Table 7 shows the composition of the reaction mixes for each of the 10 conditions.

Table 7: The different ratios of ubiquitin variants used for the K0 titration assay.

K0 ubiquitin	K48 ubiquitin	K63 ubiquitin	E2
0%, 0 µM	100%, 10 µM	--	UBCH5B
25%, 2.5 µM	75%, 7.5 µM	--	UBCH5B
50%, 5 µM	50%, 5 µM	--	UBCH5B
75%, 7.5 µM	25%, 2.5 µM	--	UBCH5B
100%, 10 µM	0%, 0 µM	--	UBCH5B
0%, 0 µM	--	100%, 10 µM	UEV1:UBC13
25%, 2.5 µM	--	75%, 7.5 µM	UEV1:UBC13
50%, 5 µM	--	50%, 5 µM	UEV1:UBC13
75%, 7.5 µM	--	25%, 2.5 µM	UEV1:UBC13
100%, 10 µM	--	0%, 0 µM	UEV1:UBC13

Apart from this, the usual ubiquitination procedure was followed using HSPA1A wt and pure Tau. The reaction time was 4 hours.

Tau ubiquitination with HSPA1A dEEVD

This assay aims to investigate the influence of the C-terminal EEVD motif of HSPA1A on the ubiquitination of Tau. For this, two separate ubiquitination reactions were performed following the usual procedure, one with HSPA1A wt and the other with HSPA1A dEEVD. Apart from that, UEV1:UBC13, ubiquitin wt and pure Tau were used. Samples were taken at several time points during a 16-hour reaction.

Determination of the affinity of NBR1 and p62 to specifically linked ubiquitin chains

For this experiment, two separate ubiquitination reactions were performed with either K48 ubiquitin and UBCH5B or K63 ubiquitin and UEV1:UBC13. For both reactions, the HSPA1A wt and pure Tau were used. The reaction volume was calculated based on the amount of bead suspension - see below. The K48 reaction took 15 minutes, and the K63 reaction took 16 hours. After the reactions were completed and the SDS samples were taken, the reactions were snap-frozen in liquid nitrogen.

Before starting to work with the anti-FLAG M2 affinity Gel A2220 (Thermo Fisher), the prey proteins were prepared in the corresponding wells of a 384-well plate (Greiner) (Table 8). For that, the prey proteins were thawed on hand, spun down at 16000 g for 10 minutes and then pipetted into the wells to reach the correct final concentration. mCherry-p62 and mCherry had a final concentration of 2 µM, while EGFP-NBR1 and EGFP were used at 1 µM. Dilutions were made with SEC buffer. The well plate was wrapped with parafilm to minimize water loss and stored at 4°C until further use.

The ubiquitination reactions were thawed on hand and then spun down at 4°C and 16000 g for 10 minutes. After thawing, the reactions were kept on ice or at 4°C. For each tested condition, 1 µl of concentrated beads was needed (For this experiment, there were six conditions – so 6 µl of concentrated beads were needed). This volume was doubled to incorporate the beads storage buffer. The total ubiquitination reaction volume (for all tested conditions combined) was calculated to saturate the amount of bead suspension used. 10 µl of anti-FLAG beads were assumed to be saturated by 6 µg of FLAG-Tau. Flag-Tau has roughly 46845 g/mol and a concentration of 1.5 µM in a ubiquitination reaction. The beads were washed trice with roughly a hundredfold volume of SEC buffer, each time vortexing for 5 seconds and spinning down at 4°C and 7000 g for 60 seconds (mixing and centrifugation settings remained unchanged throughout the assay). After removing the supernatant after the last wash, the volume of the beads was estimated using a reference tube filled with water. SEC buffer was added to the beads 1:1 to dilute them, and the beads were split into two equal fractions. The two different ubiquitination reactions (bait reactions) were added to the respective bead fraction, followed by a 1-hour incubation at 4°C rolling. The bait incubation was succeeded by two washes with SEC buffer. A five hundredfold volume of SEC buffer plus 5 mM ATP plus 5 mM $MgCl_2$ was added to the beads, followed by another incubation for 1 hour at 4°C, rolling. Again, the beads were washed twice with SEC buffer. 1 µl of clean beads loaded with bait were added to each of the wells indicated in Table 8, which were previously prepared with the prey proteins; the surrounding wells were filled with

buffer to prevent evaporation. The content of the wells was mixed by pipetting up and down, and the well plate was then incubated overnight at 4°C, shaking lightly. Images were taken the next day with an LSM700 microscope. For EGFP and mCherry, one image per well was acquired, and for p62 and NBR1, two to three images were taken, depending on the number of beads.

Table 8: The pipetting scheme for the wells of a multi-well plate. The bead fraction used for the three different preys of the respective row can be seen in the very left column. p62 and NBR1 in the table correspond to the fluorescent versions of the proteins used in the experiment. The buffer is SEC buffer.

		1	2	3	4	5
	A	Buffer	Buffer	Buffer	Buffer	Buffer
Beads with FLAG-Tau K48 ubiquitin	B	Buffer	mCherry	EGFP	p62+NBR1	Buffer
Beads with FLAG-Tau K63 ubiquitin	C	Buffer	mCherry	EGFP	p62+NBR1	Buffer
	D	Buffer	Buffer	Buffer	Buffer	Buffer

Results

The EEVD motif of HSPA1A alters the ubiquitination pattern on Tau

To investigate and specify a possible function of the C-terminal EEVD motif of HSPA1A in Tau ubiquitination by CHIP, a variant of the protein lacking said motif was expressed and purified (HSPA1A dEEVD). The mutated chaperone was utilized in an *in vitro* ubiquitination reaction and compared to the wild-type version of the same protein. Samples were taken at several time points throughout the reaction and analyzed by SDS-PAGE and subsequent anti-FLAG Western blot.

In the Western blot, where FLAG-tagged Tau was visualized, a decrease in the intensity of ubiquitinated Tau bands could be observed when using HSPA1A dEEVD compared to the reactions with HSPA1A wt (bands within the large red boxes, Figure 6A).

To analyze this decrease in more detail, a band intensity quantification was performed with three repeats of the same experiment. The regions of interest for this analysis (red boxes, Figure 6A) were chosen to incorporate all possible ubiquitination bands. The signal output is background-corrected. The intensity values were used to calculate ubiquitination differences between the two tested conditions for each time point and repeat. For that, all ubiquitination intensities (large red boxes) were corrected against the total intensity of Tau at the respective time point (small red box + large red box). The resulting values for the dEEVD and wt samples were divided by the corresponding wt sample values (from the same time point and repeat). This yields the ubiquitination intensity as a fraction of the respective wild-type signal. The means of these fractions over all three repeats are displayed in Figure 6B. At 6 h, an outlier was detected, skewing the data. Therefore, only time points 2 h and 4 h are displayed in the graph. This analysis gives an estimation of how much Tau got ubiquitinated using HSPA1A dEEVD compared to the wt version of the chaperone. The means of the wt and deletion mutant conditions were compared by applying an unpaired two-sample t-test assuming unequal variances. The one-tailed p-values resulting from this test were below the preset significance level of 0.05 (Figure 6B). Thus, a significant decrease in Tau ubiquitination upon lack of the EEVD motif could be detected after 2 h and 4 h of the *in vitro* ubiquitination reaction.

Since an influence of the EEVD motif on Tau ubiquitination could be detected via Western blot and band intensity quantification, the next step was to characterize said influence more closely in terms of targeted lysine residues. For this, a mass spectrometry analysis was performed with SDS gels from the same three experimental repeats. The gel slices used for the analysis were chosen to contain the three ubiquitination bands

between UBA1 and HSPA1A, reducing the contamination with non-Tau proteins and containing enough protein of interest to allow for MS analysis (red boxes, Figure 6C). Only one time point (4 hours) was tested. The analysis of the lower molecular weight bands of ubiquitinated substrate (compared to the higher molecular weight ubiquitination smear above UBA1) at only one time point was considered sufficient to determine whether differences in ubiquitination sites and levels could be found via MS.

The intensities of the ubiquitination signals for each modified lysine that could be detected on Tau are displayed in a bar diagram (Figure 6D). While a high variability in ubiquitination intensities between the different repeats can be observed, it is evident that a change in targeted lysine residues happened upon EEVD deletion. Three ubiquitination sites were found on Tau when using HSPA1A wt – lysine 240, 267 and 369/370. Only one of these sites (lysine 240) was modified using HSPA1A dEEVD.

In conclusion, using HSPA1A dEEVD in an *in vitro* ubiquitination reaction yielded a significantly weakened ubiquitination of Tau and, particularly, a reduction of ubiquitination sites.

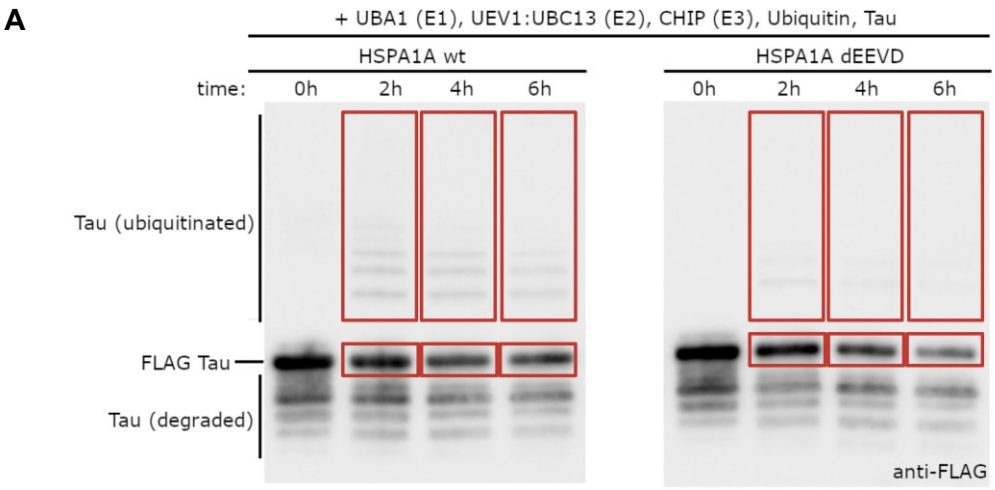
A
+ UBA1 (E1), UEV1:UBC13 (E2), CHIP (E3), Ubiquitin, Tau
HSPA1A wt
HSPA1A dEEVD
time:
0h
2h
4h
6h
Tau (ubiquitinated)
FLAG Tau
Tau (degraded)
anti-FLAG

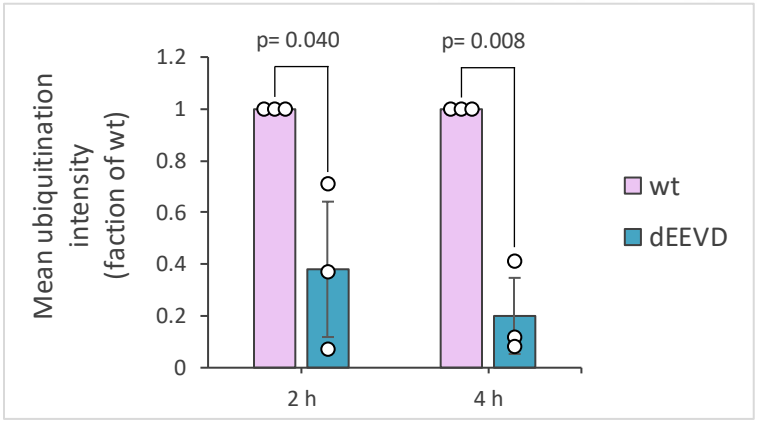
B
p= 0.040
p= 0.008
Mean ubiquitination intensity (faction of wt)
1.2
1
0.8
0.6
0.4
0.2
0
2 h
4 h
wt
dEEVD

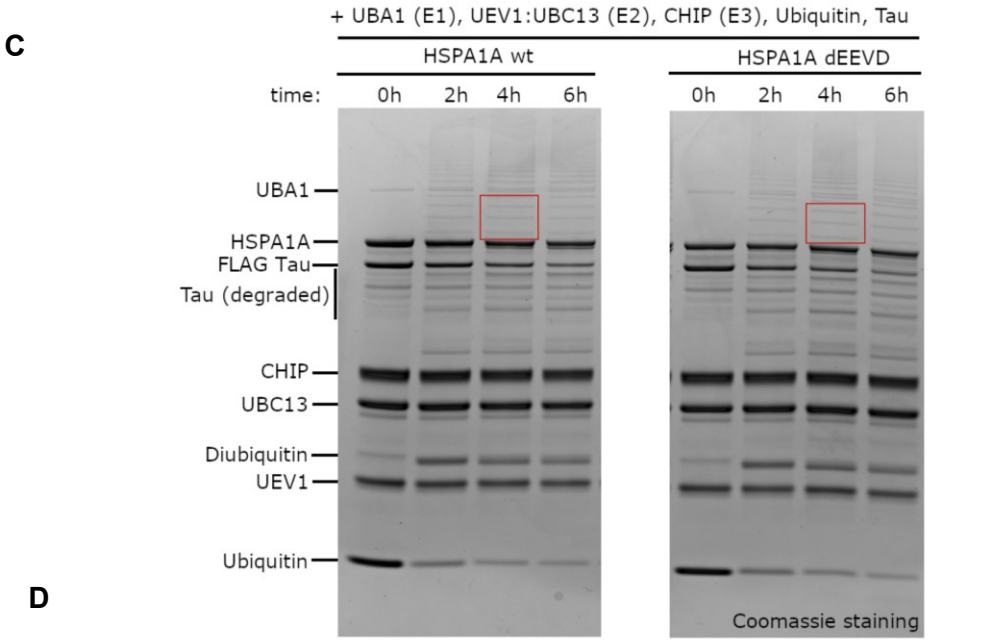
C
+ UBA1 (E1), UEV1:UBC13 (E2), CHIP (E3), Ubiquitin, Tau
HSPA1A wt
HSPA1A dEEVD
time:
0h
2h
4h
6h
UBA1
HSPA1A
FLAG Tau
Tau (degraded)
CHIP
UBC13
Diubiquitin
UEV1
Ubiquitin
Coomassie staining

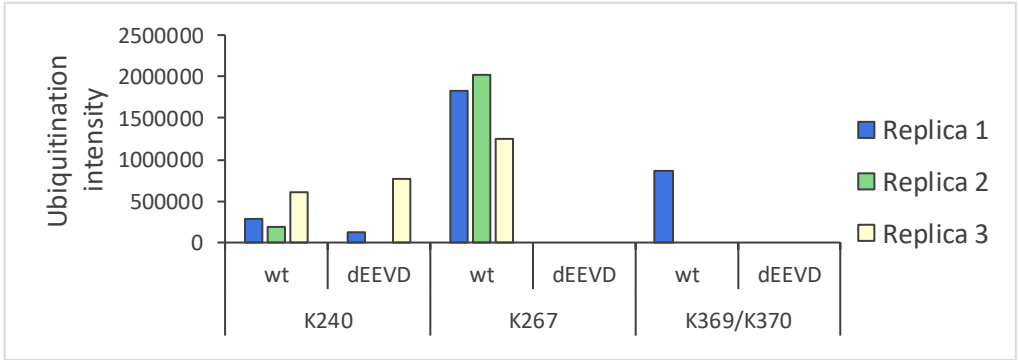
D
Ubiquitination intensity
2500000
2000000
1500000
1000000
500000
0
wt
dEEVD
wt
dEEVD
wt
dEEVD
K240
K267
K369/K370
Replica 1
Replica 2
Replica 3

Figure 6: ***(A)*** *A Western blot of a ubiquitination reaction using either wt HSPA1A (left blot) or HSPA1A dEEVD (right blot). Samples from multiple reaction times are shown. The areas used for the band intensity quantification (shown in (B)) are highlighted in red.* ***(B)*** *A band intensity quantification of the bands that are highlighted in (A). The intensity values from the large and small red boxes were added up for each time point and used as the total intensity value for Tau in the respective sample. Ubiquitination intensities were corrected against the total Tau intensities at each time point. The fraction of ubiquitination intensity was calculated as a ratio of the wt sample taken at the same time point and during the same experimental repeat. Ubiquitination intensities (fraction of wt) = (large red box intensity dEEVD or wt / (Large red box intensity dEEVD or wt + small red box intensity dEEVD or wt)) / (large red box intensity wt / (large red box intensity wt + small red box intensity wt)). The results of this calculation are depicted as a bar diagram showing the means over all three repeats for time points 2 h and 4 h. The 6 h results are not shown due to an outlier skewing the data. The bars for wt and dEEVD are magenta and cyan, respectively. The values of individual repeats are depicted by dots and the standard deviation is shown as an error bar. The one-tailed p-values, resulting from unpaired two-sample t-tests assuming unequal variances, are displayed above the bars representing each time point. The significance level is 0.05, and the difference between means for 2 h and thereby significant.* ***(C)*** *An SDS gel from the same experiment, stained with Coomassie Brilliant Blue stain. The highlighted ubiquitination bands at 4h were further analyzed by mass spectrometry. For more information on the proteins involved and the ubiquitination assay, view the methods section of this thesis.* ***(D)*** *The results from the mass spectrometry analysis of the gel slices that are highlighted in (C). The Y-axis displays the intensity of each residue on Tau that was modified by ubiquitin attachment. The three repeats are displayed in different colors. dEEVD and wt represent the version of HSPA1A used in the respective samples. When using wt HSPA1A, two ubiquitination sites could be safely assigned to K240 and K267. One additional site could be detected, which had an equal chance of being located at K369 and K370 and could, therefore, not be assigned safely to one particular lysine residue in Tau. When using the dEEVD variant, only the ubiquitination site at lysine 240 could be found.*

Controlled ubiquitin chain growth on Tau using K0, K48 and K63 ubiquitin variants

After refining our understanding of the chaperone-dependent ubiquitination of Tau, the system was harnessed to build more specific ubiquitin chains. Fewer variations in the reaction output should allow for studying the consequences of ubiquitin attachment on Tau in a more controlled manner. For example, the interaction of modified Tau with the autophagy machinery or the UPS could be studied more precisely if Tau were modified with more specific ubiquitin chains. The focus was on controlling ubiquitin chain length and linkage as they are the two main factors causing variability in the product of a ubiquitination reaction. Additionally, those two variables have proven significant for the cell's interpretation of ubiquitin signals (Finley et al., 1994; Lutz et al., 2020; Tan et al., 2008).

To control chain type and length, the K48 and K63 ubiquitin variants were used in an *in vitro* ubiquitination reaction and K0 ubiquitin was titrated into the reaction. The development of a K0 titration aimed at prematurely stopping the ubiquitin chain growth of K48- or K63-linked chains on Tau, ideally leading to the formation of short chains with specific linkages. The general functionality of the ubiquitin mutants is shown in Figure 2. Tau was ubiquitinated with either K48 ubiquitin and the E2 enzyme UBCH5B (builds preferentially K27, K48 and K63 chains if combined with CHIP+HSPA1A (Qiu, 2021)) or K63 ubiquitin and the E2 enzyme dimer UEV1:UBC13 (builds preferentially K63 chains if combined with CHIP+HSPA1A (Qiu, 2021)), aiming at specific linkage formation. Increasing concentrations of K0 ubiquitin were added to those reactions, while the concentration of the other ubiquitin mutant in the mix (K48 or K63) was steadily decreased. This should grant a measure of control over ubiquitin chain lengths by leading to premature ubiquitin chain termination or, in the case of 100% K0 ubiquitin, no buildup of chains.

Samples from each condition (different K0/K48 or K63 ratios) were taken after 4 hours and analyzed by SDS-PAGE to check whether the ubiquitination reactions worked adequately and to observe any effects the ubiquitin mutants might have had on substrate ubiquitination (Figure 7A). On the gel, an influence of K0 ubiquitin on the reaction is visible for both K48- and K63-linked chains. For K48 ubiquitin, the smear on the top part of the gels became weaker with increasing relative amounts of K0 ubiquitin, indicating a decrease in chain length (indicated by the dashed red line, Figure 7A). The smear was not expected to vanish entirely since the monoubiquitination of several different sites on Tau simultaneously (multi-monoubiquitination) should produce a similar smear (Tau - isoform 2N4R - contains 44 lysine residues, of which 22 got

ubiquitinated during these experiments, Figure 7B). For K63 ubiquitin, the first ubiquitination band above HSPA1A (indicated by a red arrow, Figure 7A) got more intense as more K0 ubiquitin was used. This indicated increased short-chain or monoubiquitin attachment on Tau when higher relative amounts of K0 ubiquitin were used since longer chains should have run higher on an SDS gel. Additionally, the diubiquitin band (labeled in Figure 7A), typically visible when using UEV1:UBC13, vanished almost completely when 100% K0 ubiquitin was applied, indicating its correct functionality. Therefore, the SDS gel suggested a shortening effect of the K0 mutant on the ubiquitin chain lengths and confirmed the successful usage of the ubiquitin variants in ubiquitinating Tau.

Next, a more detailed analysis of the targeted lysine residues and the chain linkages in ubiquitinated Tau was performed (Figure 7B&C). For that, an MS analysis was employed, focusing only on the K48/K0 samples. The bands for the analysis were chosen as in the chapter above, between the bands of UBA1 and HSPA1A (red boxes, Figure 7A). Those low ubiquitination bands were the most abundant and, therefore, the most likely to give reliable signals in MS. Additionally, those bands were considered sufficient to detect specific linkages (K48) or the absence of ubiquitin-ubiquitin linkages when using K0 ubiquitin. Two repeats of the K0 titration (samples for 100% K0 and 100 % K48 each) were analyzed by MS, determining ubiquitination target sites on Tau and ubiquitin chain linkage types (Figures 7B&C). 22 lysine residues modified with ubiquitin were detected for both 100% K0 and 100% K48 ubiquitin (Figure 7B), which is consistent with previous findings from our lab. As anticipated by the SDS gel, the number of sites modified on Tau did not decrease due to K0 ubiquitin usage. Additionally, using only K0 ubiquitin resulted in a higher intensity for most of the modified residues (corresponding to the number of Tau proteins modified at the respective residue). This is in agreement with the chain length restricting function of K0 ubiquitin. Indeed, a ubiquitin variant without lysine residues should not be able to build chains; in turn, this could lead to more enzymatic capacity being channeled towards (multi-)monoubiquitinating an increasing number of Tau proteins instead of elongating the chains on already ubiquitinated Tau. This should lead to a higher intensity value for the ubiquitinated residues on Tau, as observed.

Then, the types of chains assembled on Tau were analyzed. Different intensities for K48 linkages were found in the submitted gel slices, corresponding to the varying amounts of this particular ubiquitin-ubiquitin linkage present in the different samples. A trend towards less K48 chain formation when only K0 ubiquitin was used is evident from a table displaying the intensity values determined by MS (Figure 7C). Although the condition 100% K0/0% K48 showed a signal for K48 linkages, the signal intensity

was roughly 100 times lower than for the 100% K48 samples and could, therefore, have been a simple contamination with K48-linked chains from previous measurements. The bar diagram in Figure 7C displays this in more clarity. It depicts the means of the K48 linkage intensities as fractions compared to the 100% K48 condition. The difference between the means of the two conditions analyzed was investigated using an unpaired two-sample t-test assuming unequal variances and a significance level of 0.01. A significant decrease in K48 linkage detection could be observed when only K0 ubiquitin was available during an *in vitro* ubiquitination reaction. This aligned with a chain-shortening and chain-terminating function of K0 ubiquitin and, additionally, confirmed the K48 ubiquitin mutant's functionality since MS could detect no linkages besides those at lysine 48.

To sum up, a shortening effect of increasing amounts of K0 ubiquitin on ubiquitin chains built on Tau could be observed via both Coomassie staining (K48- and K63-linked chains) and MS (K48-linked chains), while the choice of target sites on Tau remained relatively unchanged. In addition, using the K48 ubiquitin variant yielded only K48-linked ubiquitin chains, confirming its functionality.

A

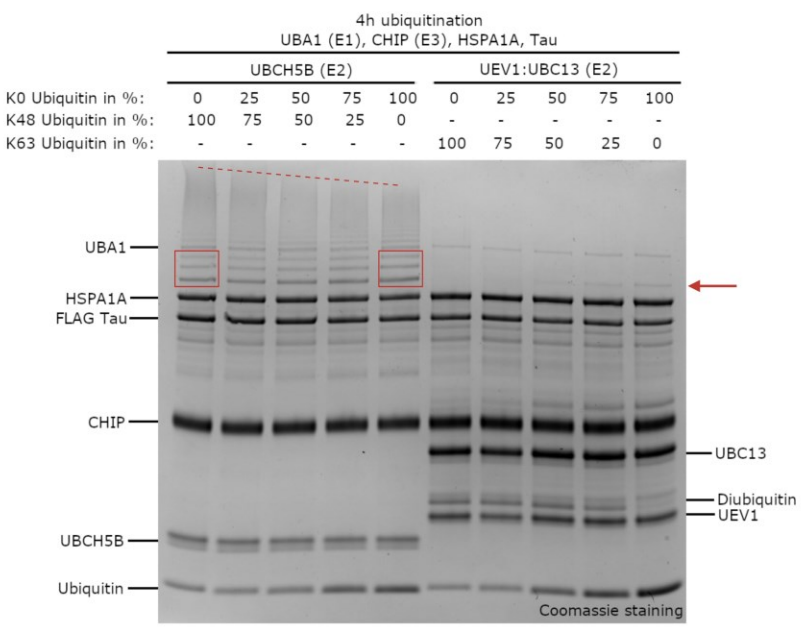

B

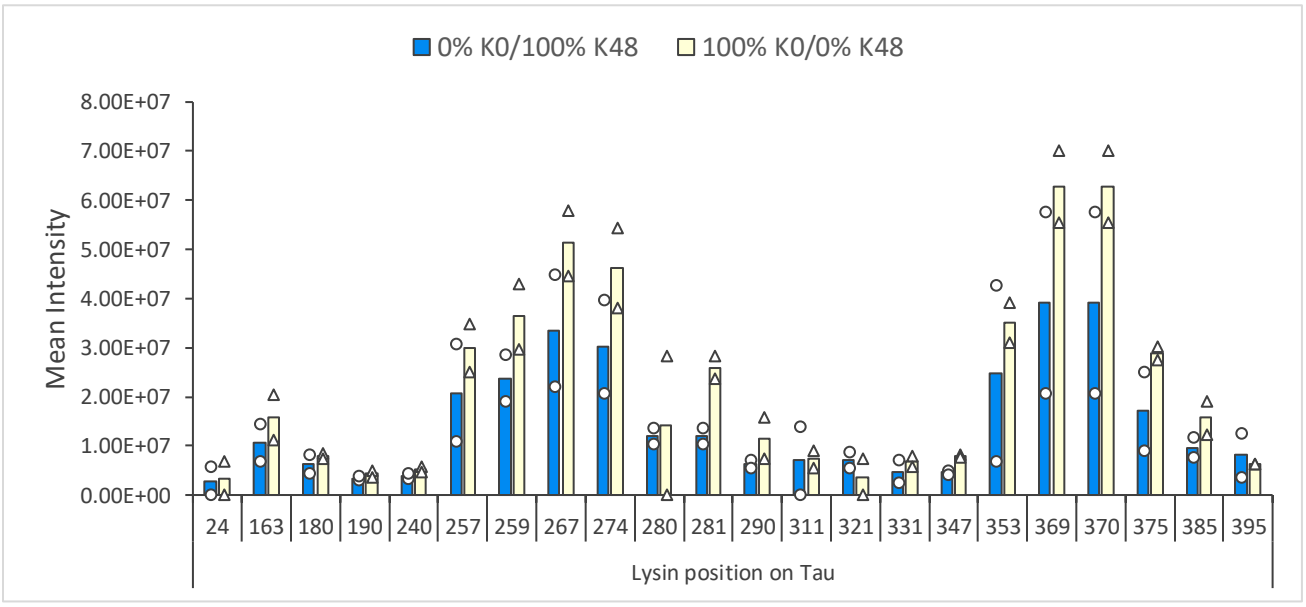

C

	K48 linkage signal intensity	
	Replica 1	Replica 2
0% K0/ 100% K48	1150000000	531000000
100% K0/ 0% K48	7920000	6510000

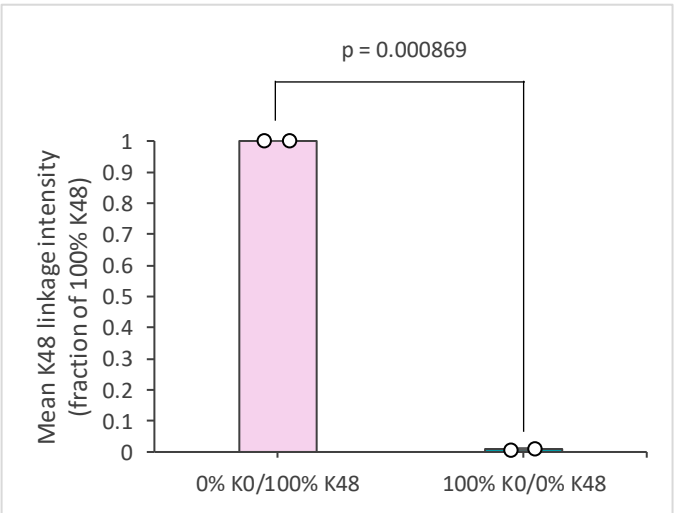

Figure 7: ***(A)*** *An SDS gel stained with Coomassie Brilliant Blue stain. It is one of three repeats from the K0 titrations. All proteins required for the ubiquitination reaction are labeled. The left half of the gel contains the reactions for K48 linked chain formation using the E2 ubiquitin-conjugating enzyme UBCH5B on K0 and K48 ubiquitin combined in different ratios. The right half of the gel contains the reactions for K63 linked chain formation using the E2 dimer UEV1:UBC13 on K0 and K63 ubiquitin combined in different ratios. The dotted red line highlights the decreasing ubiquitination smear when increasing the relative amount of K0 ubiquitin compared to K48 ubiquitin. The red arrow highlights the band for mono- or short-chain ubiquitination, which grows more intense using increasing relative amounts of K0 ubiquitin compared to K63 ubiquitin. The distinct ubiquitination bands between HSPA1A and UBA1 at 0% K0/100% K48 and 100% K0/0% K48 (in the red boxes) were cut out from the gels and sent to mass spectrometry for further analysis.* ***(B)*** *The mean intensities of the ubiquitin modifications of lysin residues on Tau over the two repeats analyzed by MS displayed in a bar diagram. The two tested conditions (red boxes in (A)) are displayed in blue and yellow. The mean intensity over the two repeats tested corresponds to the average number of Tau proteins modified at the respective lysine residue for each condition. For the condition 100% K48 the single values are depicted as circles, for 100% K0 they are triangles. The y-axis is scaled differently from 0 to 1.00E+07 and from 1.00E+07 upward.* ***(C)*** *Values of K48 linkage intensity detected by MS for each of the two tested conditions are displayed in a table on the left. Although K48 linkages could still be detected in the 0% K48 samples, the intensities for this condition are a hundredfold lower. The bar diagram on the right displays the means of the same values as fractions of the 100% K48 condition intensity. Mean K48 linkage intensity (fraction of 100% K48) = mean 0% K0/100% K48 intensity or mean 100% K0/0% K48 intensity / mean K0/100% K48 intensity. The difference of means between the two tested conditions was found significant with a one-tailed p-value of 0.000869 (shown above bars) resulting from an unpaired two-sample t-test assuming unequal variances and a significance level of 0.01. Values from the individual repeats are displayed as dots and standard deviations are shown as error bars.*

NBR1 and p62 display a binding preference for K48- over K63-linked ubiquitin chains on Tau

After producing specifically linked ubiquitin chains on the physiological substrate Tau, the role of ubiquitin linkages in autophagy could be studied. K63-linked ubiquitin chains are believed to be the primary signal for protein degradation via the autophagy-lysosome pathway compared to K48-linked ubiquitin chains (Komander & Rape, 2012).

To investigate this, the binding of the autophagy cargo receptors p62 and NBR1 to either K48-linked or K63-linked ubiquitin chains was determined. Two of the ubiquitin mutants mentioned above (K48 and K63) were used together with the respective E2 enzyme (UBCH5B, UEV1:UBC13) to build ubiquitin chains of specific linkage types on FLAG Tau. Since UEV1:UBC13 has proven to build chains much slower than UBCH5B (Qiu, 2021), the ubiquitination reaction times for the two enzymes were adjusted to ensure a relatively equal amount of ubiquitin chains on Tau for the two conditions tested (Figure 8A). A reaction time of 15 minutes for UBCH5B and 16 hours for UEV1:UBC13 resulted in a comparable amount of ubiquitinated protein once it was bound to anti-FLAG beads (red boxes in Figure 8A mark the Tau bands bound to the beads for both conditions and each repeat; the faint smear above them is the ubiquitinated protein).

The beads bound to K48- or K63-linked chains on Tau were then incubated with fluorescent mCherry-p62 and GFP-NBR1. Incubations were also performed with mCherry and GFP alone to control for unspecific binding of the fluorescent tags to the beads. The analysis was performed with a confocal microscope, detecting the intensity of fluorescent outlines around the beads (Figure 8B). The intensity of the fluorescent rings corresponds to the affinity either of the cargo receptors had for the different chain types on Tau. The images for GFP-NBR1 and mCherry-p62 clearly showed less fluorescence when K63-linked ubiquitin chains on Tau were used, while the controls remained undetectable. K48-linked chains gave a stronger signal for both GFP-NBR1 and mCherry-p62 binding.

The bead's fluorescence intensity was quantified and displayed in a box-plot diagram in Figure 8C. The diagram shows a significantly stronger binding of NBR1 and p62 to the beads coated with Tau modified with K48-linked chains compared to the beads coated with K63-linked chain-modified Tau. As a significance value, the FDR (false discovery rate) modified p-value (denoted FDR in Figure 8C) is displayed for each cargo receptor. With values below the preset significance level of 0.01, the difference in binding affinity for K48- and K63-linked chains on Tau proved to be statistically significant

for both NBR1 and p62.

In summary, under the applied experimental conditions, both tested cargo receptors displayed stronger binding to Tau modified with K48-linked ubiquitin chains compared to Tau modified with K63-linked ubiquitin chains.

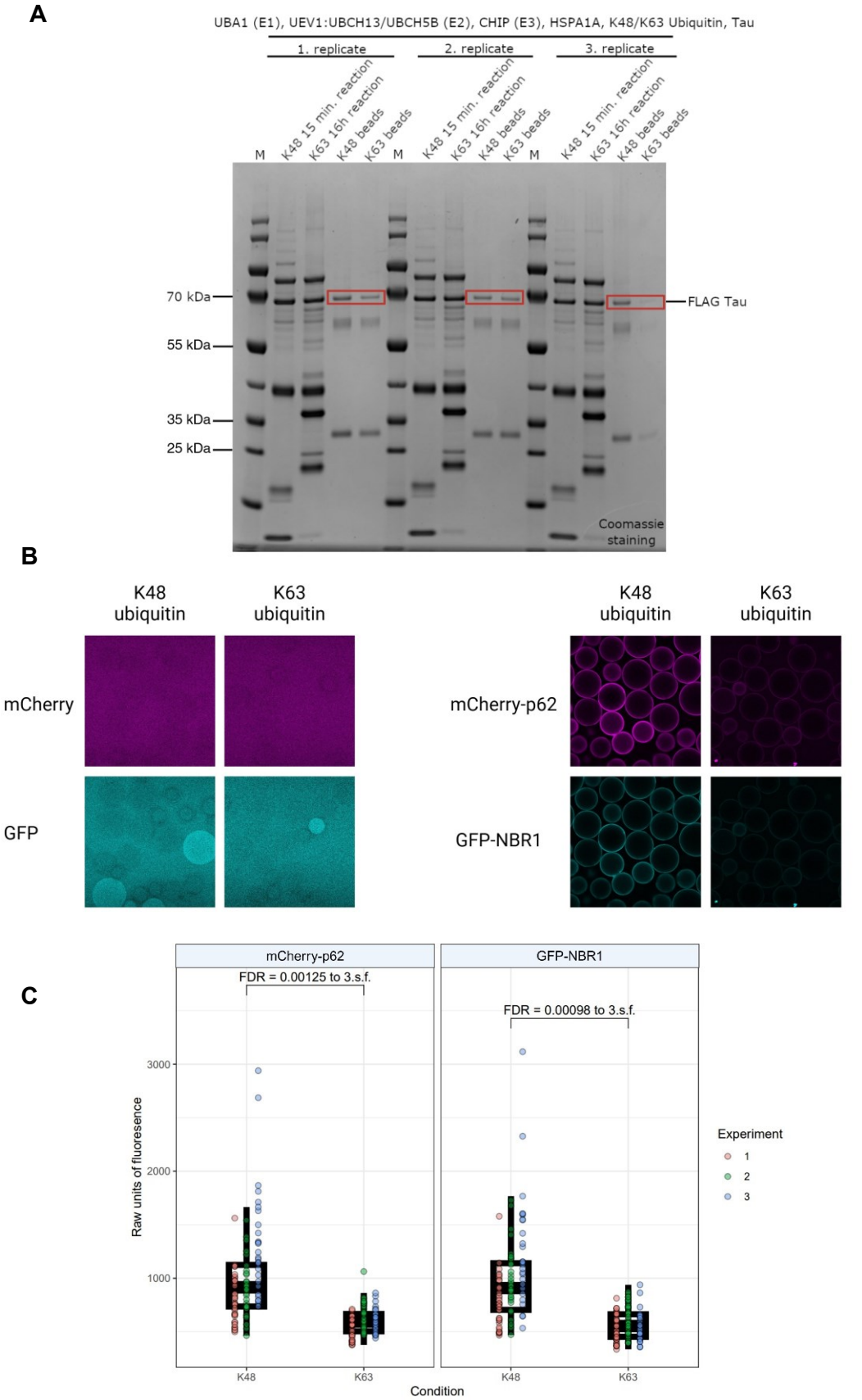

Figure 8: ***(A)*** *A Coomassie-stained SDS gel displaying the products from the time-optimized ubiquitination reactions for both K63-linked and K48-linked ubiquitin chains. The bands of Tau were highlighted in red boxes for each repeat to allow the comparison of the amount of ubiquitinated Tau bound to the beads. The bands of Tau (in the red boxes), as well as the faint smear of ubiquitination above them, should have a relatively equal intensity between the two conditions of each repeat to allow a meaningful affinity analysis of the beads under the microscope. All three repeats of the experiments are shown. The unlabeled bands that are visible below Tau at around 60 kDa and around 30 kDa are most likely the heavy and light chains of the anti-FLAG M2 antibody that is part of the anti-FLAG M2 affinity gel used in this assay.* ***(B)*** *Example microscopy images of the anti-FLAG beads bound to K48-linked or K63-linked chains on Tau. On the left, control images are shown where the beads were incubated with GFP (cyan) or mCherry (magenta), Which were not associated with the cargo receptors. As expected, the beads show no significant inherent affinity for either of the fluorescent molecules alone, and the two bead fractions attached to different chain types behave comparably. Any binding of cargo receptors to the beads can, therefore, be attributed to the affinity of the respective cargo receptor itself. On the right, mCherry-p62 affinity is displayed in magenta and GFP-NBR1 affinity in cyan.* ***(C)*** *A Box-plot diagram displaying the raw intensity of the fluorescent rings formed by mCherry-p62 and GFP-NBR1 in the presence of K48-linked or K63-linked ubiquitin chains on Tau. Every data point represents one bead imaged under the microscope. The different colors (red, green and blue) represent the three repeats of the same experiment. FDR stands for the false discovery rate modified p-values, 3.s.f. means three significant figures (rounding). The preset significance level was 0.01. FDR values below this number mean that less than 1% of the significant results will be false positives.*

Developing a strategy to purify ubiquitinated Tau using Dynabeads and UBCJ2/FK2 antibodies

While significant progress was made in controlling ubiquitin chain assembly on Tau, the preparations of ubiquitinated Tau received so far were still impure. In this second part of the thesis, several strategies to obtain clean populations of ubiquitinated Tau will be described.

A protocol for Tau isolation after a ubiquitination reaction has been previously devised and successfully applied (purification of Tau via M2 anti-FLAG beads (Qiu, 2021)). The protocol was incorporated in this work and, additionally, a focus was on eliminating the fraction of monomeric Tau (Tau without ubiquitin) and isolating Tau with relatively short ubiquitin chains. This should lead to fewer variations in the purified Tau species (reasons for isolating only shorter ubiquitin chains are explained in more detail in the chapter "Controlled ubiquitin chain growth on Tau using K0, K48 and K63 ubiquitin variants" and in the discussion).

Approaches using bead-based purification strategies, in combination with either ubiquitinated protein conjugate-specific antibodies or TUBEs (tandem ubiquitin-binding entities), are described in this thesis. A simplified scheme summarizing the bead-based purification strategies is shown in Figure 9A. Initially, UBCJ2/FK2 antibodies (two interchangeable antibodies) against mono- and polyubiquitinated conjugates were used to isolate ubiquitinated Tau with beads. Either of the antibodies was attached to protein G Dynabeads, which were used in combination with the established Tau purification protocol via M2 anti-FLAG beads.

After performing a ubiquitination reaction (of only 1 hour or less with UEV1:UBC13 – to keep the chains on Tau relatively short), the antibody-bound Dynabeads were added to the reaction mix to specifically bind the ubiquitinated substrates in it. The eluate, containing different kinds of ubiquitinated proteins, underwent a selection for Tau via the protein's FLAG tag, which can bind to M2 anti-FLAG beads. It was possible to isolate a relatively promising eluate from the Dynabeads, meaning bands of high molecular weight comparable to those that would be expected from ubiquitinated Tau. These bands also gave a signal when stained with anti-FLAG antibodies in a Western blot (red boxes, columns 3, Figure 9B). However, the bands were lost completely whenever the buffer was adjusted from elution conditions (acidic) to conditions more suitable for subsequent usage of M2 beads (used at a neutral pH) (red boxes, columns 4, Figure 9B). Several different elution buffers and adjustment strategies were tested to resolve this problem. Unfortunately, all of them remained unsuccessful (Figures 9B-G). The anti-FLAG purification steps are therefore only displayed in Figure 9B. The different pH

adjustment strategies ranged from adding small amounts of highly concentrated single components of a buffer system one after the other (to reach the concentrations typical for SEC buffer – 25 mM HEPES, 150 mM NaCl, 1 mM DTT) (Figure 9B), additionally adding glycerol or detergent (Figure 9C), adding a large volume of ready-made buffers, like SEC buffer, (either at once or via dialysis) and then concentrating the resulting solution (Figure 9G), adjusting with buffers of different pH values (instead of 7.5) (Figure 9D) sometimes in combination with solubility increasing agents (glutamic acid, arginine (Shukla & Trout, 2011) and high salt concentrations) (Figure 9G). Also, alternative elution buffers were tested: buffers with a neutral pH (sarkosyl buffer) (Figure 9D), buffers with a less acidic pH (arginine and $MgCl_2$) (Figure 9G) or elution buffers that elute based on competitive binding of other ubiquitin species to the beads (free K63-linked chains and GST 4x ubiquitin) (Figure 9E&F).

This means that, despite extensive effort, the purification with Dynabeads did not allow the protein of interest to be retained in a neutral buffer.

A

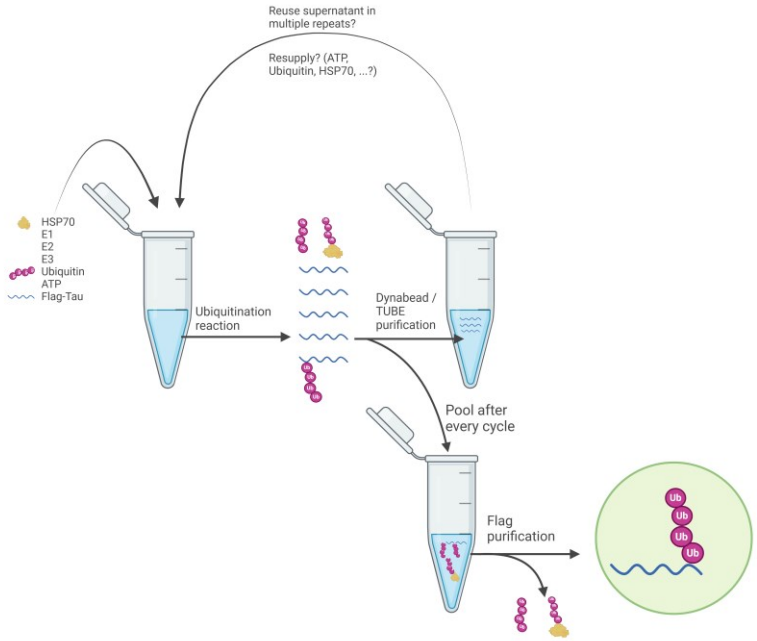

B

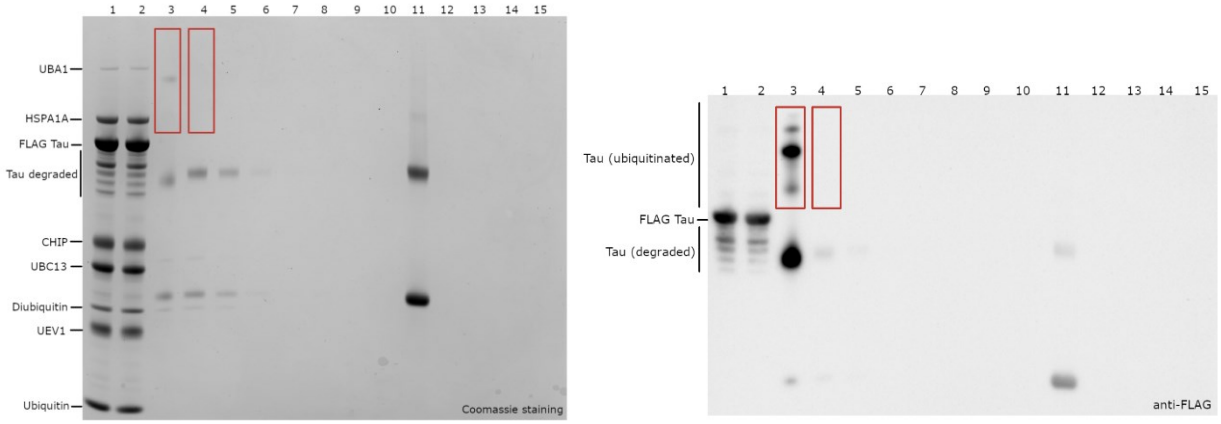

1: 30 min. ubiquitination
2: Dynabeads: Unbound
3: Dynabeads: Eluate
4: Dynabeads: Eluate+HEPES+NaCl+DTT
5: Anti Flag: Unbound
6: Anti Flag: MgCl2 ATP wash
7: Anti Flag: ATP wash
8-9: Anti Flag: Buffer wash 1-2
10: Anti Flag: eluate
11: Anti Flag: beads after elution
12-14: Anti Flag: FT 1-3 50K
15: Anti Flag: Final sample

C

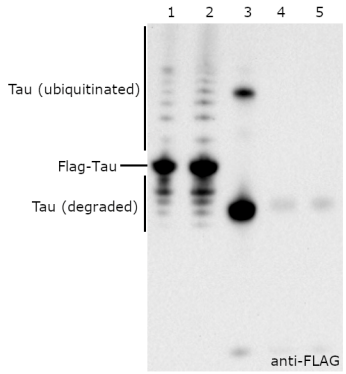

1: 1h ubiquitination
2: unbound fraction
3: Glycine buffer elution
4: Eluate + Glycerol + HEPES + High NaCl + DTT
5: Eluate + CHAPS + HEPES + NaCl + DTT

D

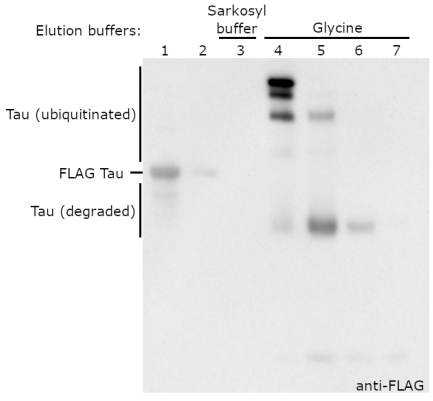

1: 1 h ubiquitination
2: 1. wash
3: Elution
4: Elution
5: Adjustment to pH 5.5 with MES buffer
6: Adjustment to pH 6.5 with MES buffer
7: Adjustment to pH 8.5 with Tris buffer

E

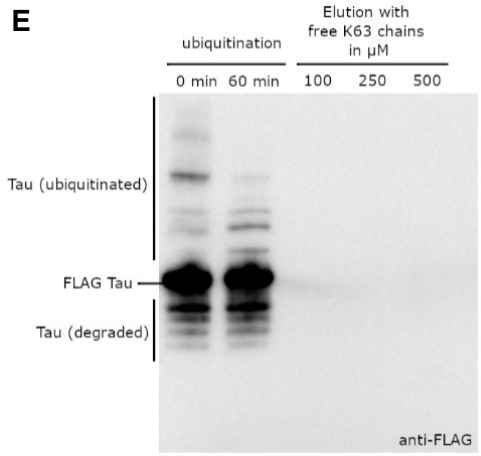

F

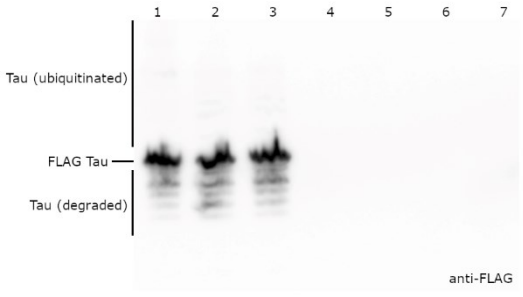

1: 0 min. ubiquitination
2: 1 h ubiquitination
3: unbound fraction
4: 50 µM GST 4x ubiquitin
5: 150 µM GST 4x ubiquitin
6: 250 µM GST 4x ubiquitin
7: 300 µM GST 4x ubiquitin

G

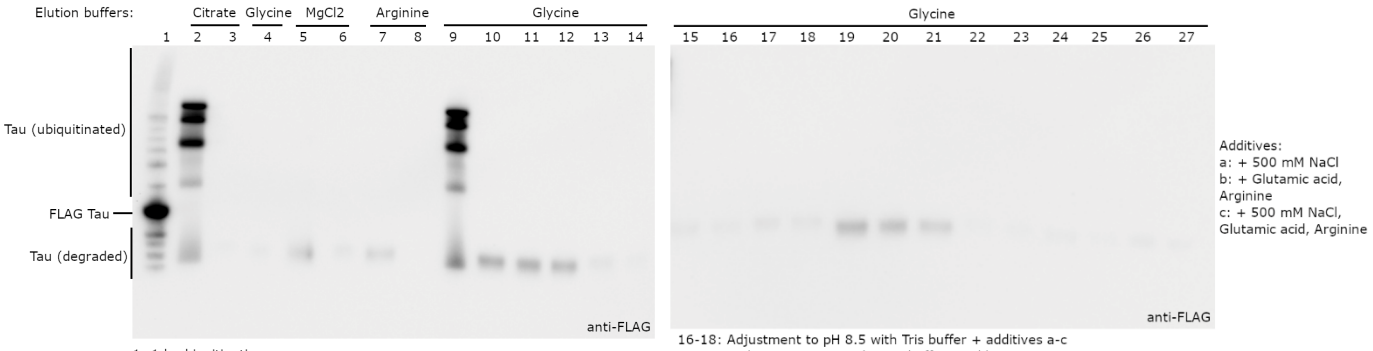

1: 1 h ubiquitination
2: Elution
3: Adjustment to pH 7.5 with SEC buffer
4: Buffer exchange to citrate buffer
5: Elution
6: Adjustment to pH 7.5 with SEC buffer
7: Elution
8: Adjustment to pH 7.5 with SEC buffer
9: Elution
10-12: Adjustment to pH 5.5 with MES buffer + additives a-c
13-15: Adjustment to pH 6.5 with MES buffer + additives a-c
16-18: Adjustment to pH 8.5 with Tris buffer + additives a-c
19-21: Dialysis to pH 5.5 with MES buffer + additives a-c
22-24: Dialysis to pH 6.5 with MES buffer + additives a-c
25-27: Dialysis to pH 8.5 with Tris buffer + additives a-c

Figure 9: ***(A)*** *A scheme explaining the purification of ubiquitinated Tau. The first step is a ubiquitination reaction over a variable time span. The second step is an isolation of all ubiquitinated components of the reaction mix via affinity to either a fitting antibody or TUBEs. The third step is further purification of the ubiquitin species by selecting for FLAG Tau via anti-FLAG beads. The big arrow on top, pointing from the first purification step to the ubiquitination reaction, demonstrates the potential option to reuse the supernatant, which, otherwise, would be discarded once the ubiquitinated proteins are bound to the beads. For reuse, any components that are being used up during the reaction could be resupplied to the supernatant, and another reaction cycle could be started. This could be repeated several times to optimize the usage of Tau, which is thought to remain largely non-ubiquitinated within only one reaction cycle. So far, this option has not been realized.* ***(B)*** *A Coomassie-stained SDS gel (left) and an anti-FLAG Western blot (right) of the same experiment (purification of ubiquitinated Tau). Several alterations of this experiment will be shown after this one, but since the Coomassie-stained gel mainly checks for correct pipetting, and since the ubiquitination reactions remain the same for each experiment in this figure, from here on, only the Western blots will be shown. Since the blot exposure was generally kept relatively low so as not to overexpose the band of monomeric Tau, and since the ubiquitination reactions for Dynabeads purifications were performed in 1h or less by UEV1:UBC13 (no strong ubiquitination so early on by this enzyme dimer (Qiu, 2021)) the bands for ubiquitinated Tau tended to be very faint or barely visible. The gel and blot show samples from several steps throughout a ubiquitinated Tau purification. The proteins bound to the Dynabeads before elution were initially checked on a Coomassie gel but were not visible probably due to low concentrations; data not shown here. More detailed information on the single steps of this process can be viewed in the Methods section of this thesis. All reaction components are labeled. The unlabeled bands that are visible on the Coomassie-stained gel at roughly the height of degraded Tau (around 50 kDa) and diubiquitin (around 25 kDa) and are also giving a weak signal on the blot were most likely the heavy and light chains of the anti-ubiquitinated proteins antibody, which seemed to partially coelute with the ubiquitinated species. Columns three show the elution from the Dynabeads with acidic glycine buffer. On the Western blot, there is one strong band and some a little less prominent ones above monomeric Tau (highlighted in red box, column 3). The height of these bands corresponds roughly to the expected weight of ubiquitinated Tau. In column four, the eluate was adjusted with small amounts of concentrated HEPES, NaCl and DTT to a neutral pH of 7.5. During buffer adjustment, the protein of interest seemed to have fallen out of solution since nothing can be seen on the blot anymore (highlighted in red box, column 4).* ***(C)*** *A Western blot of a purification with Dynabeads. In this case, the pH after elution was adjusted with a strategy similar to B, but with the addition of solubilizing agents like detergent (CHAPS) or glycerol. From here on, only the steps until the elution from the Dynabeads are shown.* ***(D)*** *A Western blot of a purification with Dynabeads. After elution, the low pH was adjusted to various pH values with either MES or Tris buffer. Additionally, in column three, a neutral pH elution buffer (sarkosyl buffer) was tried. In these cases, the ubiquitination bands were mostly or entirely lost as well.* ***(E)*** *A Western blot of a purification with Dynabeads. The elution strategy was changed from low pH elution to elution via competitive binding. Varying high amounts of free K63-linked ubiquitin chains were added as an elution buffer. The high concentration of K63-linked chains should substitute the ubiquitinated protein's bond with the antibodies on the Dynabeads and, therefore, release them.* ***(F)*** *A Western blot of a purification with Dynabeads. This time, competitive binding was attempted with varying high concentrations of GTS 4x ubiquitin.* ***(G)*** *The final Western blot of a Dynabeads purification. Citrate, $MgCl_2$ and arginine elutions were performed and adjusted with 1x SDS buffer. In column four, one fraction of the glycine elution was buffer-exchanged to citrate buffer, which has a similar pH. The rest of the blot contains only glycine elutions, which were adjusted with three different buffers at varying pH values. Each buffer was mixed with three different combinations of additives, resulting in 9 different buffers (the additives are listed on the very right of the image). All of these buffers were used for adjustment either via quick addition of a big volume and subsequent sample concentration or via slow dialysis overnight. Any details regarding different elution buffers or adjustment strategies can be viewed in the methods section of this thesis.*

Developing a strategy to purify ubiquitinated Tau using GST binding beads and GST-TUBEs

Alternative to the purification protocol described in the previous chapter, a modified strategy was developed to achieve the same goal.

In this case, GST-TUBEs (GST-linked tandem ubiquitin-binding entities) were attached to GST-binding beads and then used instead of the antibody-bound Dynabeads as the purification step, which selects for ubiquitinated substrates. TUBEs are an assembly of multiple UBA domains that can bind to polyubiquitin chains with Kds (dissociation constants) in the nanomolar range (Figure 10A). Therefore they should be able to select for ubiquitin-bound proteins after an *in vitro* ubiquitination reaction, including modified Tau. Their use in the purification of ubiquitinated Tau is depicted schematically in Figure 9A.

After removing the proteins of a ubiquitination reaction that were not bound by TUBEs, the protein of interest was eluted from the bead-associated TUBEs using a range of different buffers. This includes a $MgCl_2$ elution, which showed very weak but promising bands (cyan box, Figure 10B). The $MgCl_2$ buffer has a slightly less acidic pH than Glycine buffer (4.5 compared to 2.8), providing a more gentle elution that requires a less extreme pH change to reach neutral conditions suitable for M2 anti-FLAG beads. The pH adjustment needed for further purification of ubiquitinated Tau might, therefore, be more successful. Even though the bands from the $MgCl_2$ elution are quite faint, they are clean and discrete, showing good potential for successful downstream use. However, this would require a considerable scale-up.

In summary, none of the purification strategies led to the complete isolation of ubiquitinated Tau. The purification with TUBEs yielded a promising intermediate product but has not been continued so far (for more details, see discussion).

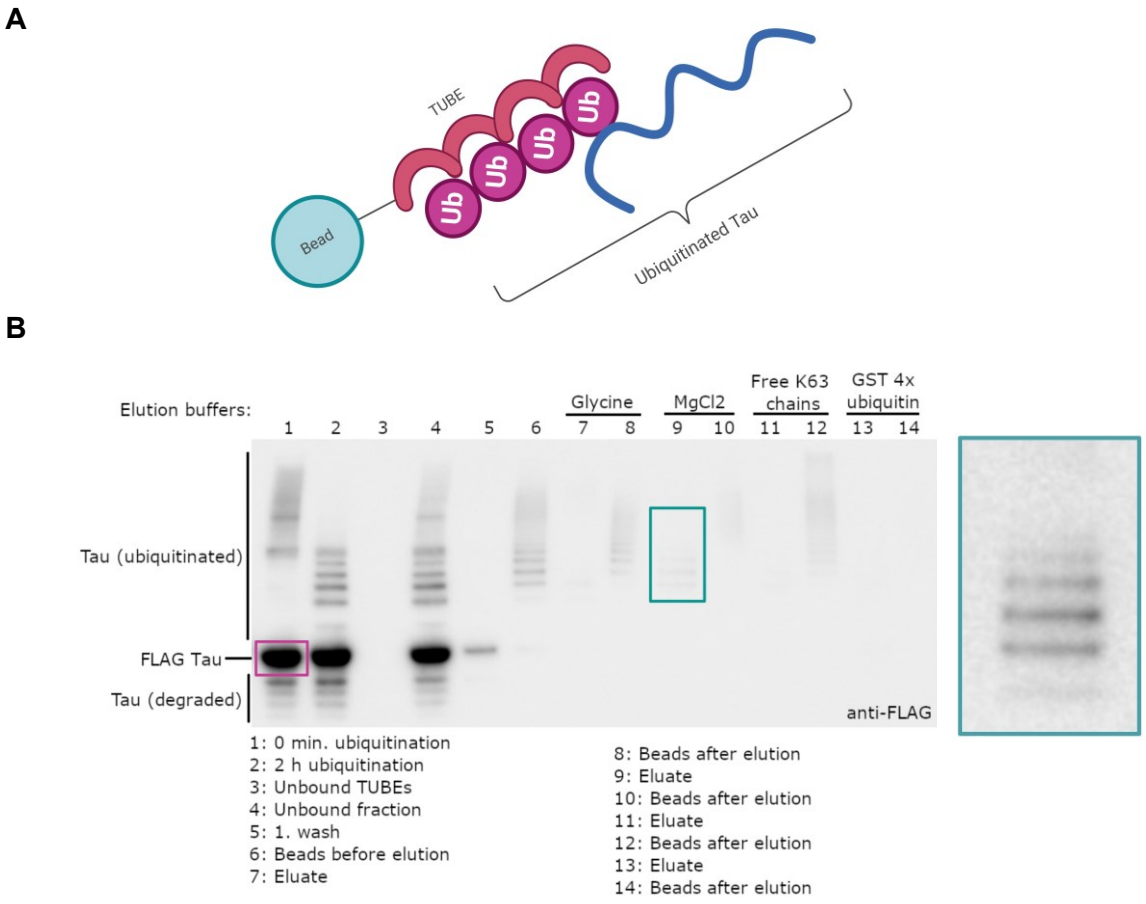

Figure 10: ***(A)*** *A scheme displaying the functionality of TUBEs. The TUBEs used in my experiments have four successive UBA domains, each capable of binding single ubiquitin molecules. Together, they exhibit a high affinity for polyubiquitin chains. When attached to beads, they can be used to pull down and isolate ubiquitin or ubiquitinated proteins (here, ubiquitinated Tau).* ***(B)*** *A Western blot of a purification with TUBEs. Several elution buffers were screened (glycine buffer, $MgCl_2$, free K63-linked chains, GST 4x ubiquitin). The $MgCl_2$ elution displays bands at the correct height for ubiquitinated Tau, highlighted in cyan. This highlighted section is also shown on the very right in a zoomed-in state and from a slightly overexpressed anti-FLAG Western blot. The FLAG Tau band is highlighted in pink. Both highlighted parts of the blot were analyzed by band intensity quantification and used to estimate the pure ubiquitinated Tau yield; described in the discussion. Any details regarding different elution buffers or adjustment strategies can be viewed in the methods section of this thesis.*

Discussion

This thesis aimed to investigate and improve different aspects of the *in vitro* ubiquitination of Tau and to dissect Tau's interaction with the autophagy machinery. More specifically, the role of HSPA1A's EEVD motif in Tau ubiquitination was investigated. Additionally, the development of a strategy to produce more length- and linkage-specific ubiquitin chains on Tau was initiated by applying particular ubiquitin mutants. The resulting specifically linked ubiquitin chains on Tau were used to investigate ubiquitin chain linkage-specific cargo binding by autophagic cargo receptors. And lastly, the purification of ubiquitinated Tau was further developed.

Investigating the C-terminal EEVD motif of HSPA1A and its role in Tau ubiquitination revealed a significantly weaker ubiquitination activity and a reduced number of ubiquitination sites on Tau when HSPA1A lacked said motif.
CHIP, the E3 ubiquitin ligase used in Tau ubiquitination assays, is a TPR-containing protein that was shown to interact with HSP70 family proteins via their EEVD motif (Smith et al., 2013; Zhang et al., 2015). It could be demonstrated that CHIP ubiquitinates Tau (Petrucelli et al., 2004) and, although sources disagree on the matter, HSP70 proteins have been implicated as important factors in the ubiquitination of Tau by CHIP (Shimura et al., 2004). It was proposed that HSP70 proteins might bind to their substrates first and that the resulting complex is then recognized by CHIP for subsequent ubiquitin attachment (Quintana-Gallardo et al., 2019; Shimura et al., 2004). Since the interaction of HSP70 and CHIP is lost upon EEVD deletion (S.-J. Wu et al., 2001), I assumed that any guiding or supporting function HSP70 might provide for the E3 ligase would be lost in the absence of this motif as well. The reduction in the number of different lysine residues modified on Tau when using HSPA1A dEEVD (Figure 6D) aligns well with this assumption. Especially the loss of K267 ubiquitination supports this model since this residue is very close to an identified HSP70 protein binding site on Tau (Sarkar et al., 2008). If HSPA1A acts as a guide for the E3 ligase CHIP to specific residues on Tau, it could be reasonably expected that ubiquitination of Tau in close proximity to an HSP70 binding site would be lost or decreased upon prevention of chaperone cochaperone association. This theory implies that HSP70 proteins are not explicitly required for efficient Tau ubiquitination by CHIP - in alignment with a study by Munari et al. (2022) - but might be critical for targeting ubiquitination to specific residues on Tau.
While the results allow for such interesting conclusions, they should be backed up with

adjacent experiments further confirming and investigating the relevance of an association between HSP70 and CHIP for targeting specific sites on Tau. For instance, related assays could leave the interaction between HSP70 and CHIP intact, instead targeting the association between HSP70 and Tau. Tau contains binding sites for HSP70 (Sarkar et al., 2008) and altering those by mutagenesis should compromise the HSP70-Tau interaction. The binding site mutant's effects on ubiquitination could subsequently be compared to the effects triggered by an EEVD motif loss. This would clarify whether HSP70 serves as a guide for targeted ubiquitination since that should require physical interaction with both the E3 ligase and the substrate. Experiments like this could shed more light on the mechanism underlying Tau ubiquitination and its subsequent degradation. Additionally, corresponding in-cell experiments could be performed to back up the *in vitro* data. The data acquired so far represents only the starting point of an exciting research path toward a more in-depth understanding of HSP70:CHIP-based substrate ubiquitination.

Experiments using K0, K48 and K63 ubiquitin variants could confirm the functionality of K48 ubiquitin and could attribute a chain-shortening effect to K0 ubiquitin.
Studies applying the K0 ubiquitin variant could also observe a chain-restricting effect in enzymatic *in vitro* ubiquitination assays analyzed via Western blot (Richard et al., 2020; G. Wang et al., 2024). In both studies, some ubiquitination smear was visible when only K0 ubiquitin was available to the reaction. Richard et al. (2020) explained the remaining bands with multi-monoubiquitination. This is a likely explanation for the remaining ubiquitination bands also in the case of this work since multiple lysine residues on Tau were shown to be ubiquitinated by UBCH5B, chaperone-assisted CHIP and K0 ubiquitin (Figure 7B). This suggests that K0 ubiquitin indeed terminates ubiquitin chain elongation. In this thesis, an additional analysis was performed using MS. There, a signal for K48 linkages could be detected in samples containing only K0 ubiquitin. However, the signal intensity was only about 1% of that from samples containing only K48 ubiquitin (Figure 7C). Therefore, it can most likely be attributed to impurities in the spectrophotometer, which supports the correct functionality of K0 ubiquitin.
To further verify this, a Western blot using chain-specific antibodies should be performed to safely exclude the possibility of K48 linkages in samples with only K0 ubiquitin.
These results suggest that using K0 ubiquitin might allow controlling ubiquitin chain length to a certain extent. So far, the length of ubiquitin chains has been virtually unrestricted during our *in vitro* ubiquitination assays. Although precise ubiquitin chain

length control during enzymatic ubiquitination assays by using K0 ubiquitin seems unlikely, the results of this thesis suggest that a more general chain length restriction could be possible. Producing Tau modified with shorter ubiquitin chains represents a considerable improvement over no chain length control. Firstly, because the product variability would be reduced, and secondly, because Tau modified with relatively short ubiquitin chains could represent a more physiologically relevant research subject. This is in line with a study by Tsuchiya et al. (2018), which has found ubiquitin chains in yeast cell lysates to be on average not more than 7 units long. This study aligns well with our aim to restrict unlimited chain growth in ubiquitination assays.

The third ubiquitin mutant that was produced (K63 ubiquitin) has yet to be tested for specific chain formation. As a follow-up experiment, I suggest specific K63-linked ubiquitin chain formation on Tau using K63 ubiquitin and UEV1:UBC13 and subsequent analysis by MS. The specificity of K48- and K63-linked ubiquitin chains could then be additionally confirmed using a chain-specific Western blot, as mentioned above.

Successfully producing specific ubiquitin chains could allow for future experiments with highly defined substrates. That would mean excluding effects caused by random linkage types (and chain lengths) and permitting the assignment of results to one modification instead of many variations of a modification. This could confer more clarity, for instance, to the role of specifically linked ubiquitin chains in pathways like autophagy or the UPS. It might aid in further investigating the roles of K48- and K63-linked ubiquitin chains in channeling targets towards either of the two pathways, as described in the paragraph below. In general, more precise and meaningful findings could be made once specific ubiquitin chains can be successfully produced on Tau.

When investigating the affinity of the two autophagic cargo receptors NBR1 and p62 for K63-linked or K48-linked ubiquitin chains, a significantly stronger binding of both cargo receptors to K48-linked chains could be detected. This is not in alignment with the literature addressing this topic. The cargo receptor p62 was found to display a higher affinity for K63-linked ubiquitin (Tan et al., 2008; Wurzer et al., 2015), while NBR1 seems to display no evident linkage preference (Walinda et al., 2014). Most studies concerning the chain preferences of the two mentioned cargo receptors are performed with free ubiquitin chains or ubiquitin attached to artificial substrates like GST. Using specifically linked chains on the physiological substrate Tau for *in vitro* affinity analysis provides a new – possibly more meaningful – approach to the question of cargo specificity.

Two E2 enzymes, known to perform with different efficiencies (Qiu, 2021), were used to attach differently linked ubiquitin chains to Tau. The reaction times were adjusted

accordingly, and the amount of (ubiquitinated) substrate bound to the beads was checked by SDS-PAGE and found relatively similar (Figure 8A). Yet, comparing (very low) protein amounts on an SDS gel is not extremely precise and the bands of the two groups are not perfectly equal. Therefore, the heightened affinity of both NBR1 and p62 for K48-linked chains might be, in part, due to an excess of ubiquitinated substrate availability on these beads compared to beads bound by K63-linked ubiquitin chain-modified Tau. In other words, it cannot be safely assumed that all beads were equally loaded with ubiquitinated Tau or that Tau ubiquitination by K48 and K63 ubiquitin happened to a comparable extent. Therefore, a more precise determination of the amount of K48-linked and K63-linked ubiquitinated Tau bound to the beads (for instance, via western blot or mass spectrometry) would confer more meaning to the obtained results. Once the influence of variable bead-loading on the results can be excluded, the surprising preference of Tau modified with K48-linked ubiquitin chains as an autophagic cargo could be further investigated.

Concerning the isolation of ubiquitinated Tau, no complete purification has been performed so far. Instead, a purification strategy using TUBEs-bound beads and a $MgCl_2$ elution to isolate ubiquitinated proteins yielded a promising intermediate product (pH adjustment not yet checked) (Figure 10B). The bands of this elution on an SDS gel were clear and discrete and were located at a height that suggested Tau to be either (multi-) monoubiquitinated or modified by only short ubiquitin chains, as was the objective of the experiment. However, the resulting bands of pure ubiquitinated proteins were relatively faint. The experimental scale would have to be increased significantly to receive enough pure ubiquitinated Tau for usage in subsequent assays.
To illustrate this, an estimation of the current ubiquitinated Tau yield was performed:
The intensity values resulting from a band intensity quantification (the bands are highlighted in Figure 10B in pink and cyan) allowed estimating that only about 0.04% of the original Tau, which was added to the reaction, eventually got eluted from the anti-FLAG beads with $MgCl_2$.
The input of Tau for the whole reaction was roughly 9 nmol.
The estimated purification product would then be 0.0036 nmol (assuming that the whole reaction is eluted with $MgCl_2$ and that no more Tau is lost during the M2 anti-FLAG purification step)
If one wanted to obtain 100 µl of 50 µM pure ubiquitinated Tau (a reasonable product amount for a protein purification), they would have to use 125 ml of pure monomeric Tau (assuming a generous concentration of 100 µM) as a reaction substrate, which corresponds to roughly 1250 L of E. coli expression culture.

Therefore, to obtain decent amounts of pure ubiquitinated Tau, not only a scale-up of the ubiquitination reaction but also its optimization would be required.

Several improvements could be made. Firstly, the conditions for ideal Tau ubiquitination have not been screened in detail so far, and the possibility is high that more beneficial conditions can be discovered to increase the ubiquitin attachment efficiency on Tau, resulting in a higher product yield. Secondly, an E2 screen could be performed in order to discover an E2 that attaches ubiquitin to Tau more efficiently. Thirdly, reaction components that were not consumed during a ubiquitination reaction could be recycled to be used in multiple reaction cycles (Figure 9A). That means proteins not consumed or only partially consumed during a ubiquitination reaction, like Tau, could theoretically be reused in several ubiquitination cycles while only resupplying factors like ubiquitin or ATP, which are used up during a reaction. This could minimize the protein input for such a reaction while maximizing the product of interest. Fourthly, the reaction efficiency could be improved using chemically synthesized monoubiquitinated Tau as a substrate instead of non-ubiquitinated Tau. Monoubiquitination of a substrate was shown to drive its efficient polyubiquitination (K. Wu et al., 2024), a concept that could be exploited for Tau ubiquitination optimization.

Employing such optimization strategies might allow experimentally relevant amounts of pure ubiquitinated Tau to be produced. This product could form a key component of future experiments concerning protein degradation and AD, providing meaningful and unambiguous results due to its high purity.

References

Adriaenssens, E., Ferrari, L., & Martens, S. (2022). Orchestration of selective autophagy by cargo receptors. *Current Biology*, *32*(24), R1357–R1371. https://doi.org/10.1016/j.cub.2022.11.002

Arakhamia, T., Lee, C. E., Carlomagno, Y., Kumar, M., Duong, D. M., Wesseling, H., Kundinger, S. R., Wang, K., Williams, D., DeTure, M., Dickson, D. W., Cook, C. N., Seyfried, N. T., Petrucelli, L., Steen, J. A., & Fitzpatrick, A. W. P. (2020). Posttranslational Modifications Mediate the Structural Diversity of Tauopathy Strains. *Cell*, *180*(4), 633-644.e12. https://doi.org/10.1016/j.cell.2020.01.027

Bauer, B., Martens, S., & Ferrari, L. (2023). Aggrephagy at a glance. *Journal of Cell Science*, *136*(10), jcs260888. https://doi.org/10.1242/jcs.260888

Berndsen, C. E., & Wolberger, C. (2014). New insights into ubiquitin E3 ligase mechanism. *Nature Structural & Molecular Biology*, *21*(4), 301–307. https://doi.org/10.1038/nsmb.2780

Breijyeh, Z., & Karaman, R. (2020). Comprehensive Review on Alzheimer's Disease: Causes and Treatment. *Molecules*, *25*(24), 5789. https://doi.org/10.3390/molecules25245789

Ciuffa, R., Lamark, T., Tarafder, A. K., Guesdon, A., Rybina, S., Hagen, W. J. H., Johansen, T., & Sachse, C. (2015). The Selective Autophagy Receptor p62 Forms a Flexible Filamentous Helical Scaffold. *Cell Reports*, *11*(5), 748–758. https://doi.org/10.1016/j.celrep.2015.03.062

Cowan, A. D., & Ciulli, A. (2022). Driving E3 Ligase Substrate Specificity for Targeted Protein Degradation: Lessons from Nature and the Laboratory. *Annual Review of Biochemistry*, *91*(1), 295–319. https://doi.org/10.1146/annurev-biochem-032620-104421

Dickey, C. A., Yue, M., Lin, W.-L., Dickson, D. W., Dunmore, J. H., Lee, W. C., Zehr, C., West, G., Cao, S., Clark, A. M. K., Caldwell, G. A., Caldwell, K. A., Eckman,

C., Patterson, C., Hutton, M., & Petrucelli, L. (2006). Deletion of the Ubiquitin Ligase CHIP Leads to the Accumulation, But Not the Aggregation, of Both Endogenous Phospho- and Caspase-3-Cleaved Tau Species. *The Journal of Neuroscience*, *26*(26), 6985–6996. https://doi.org/10.1523/JNEUROSCI.0746-06.2006

Finley, D., Sadis, S., Monia, B. P., Boucher, P., Ecker, D. J., Crooke, S. T., & Chau, V. (1994). Inhibition of proteolysis and cell cycle progression in a multiubiquitination-deficient yeast mutant. *Molecular and Cellular Biology*, *14*(8), 5501–5509. https://doi.org/10.1128/MCB.14.8.5501

Gendron, T. F., & Petrucelli, L. (2009). The role of tau in neurodegeneration. *Molecular Neurodegeneration*, *4*(1), 13. https://doi.org/10.1186/1750-1326-4-13

Ghag, G., Bhatt, N., Cantu, D. V., Guerrero-Munoz, M. J., Ellsworth, A., Sengupta, U., & Kayed, R. (2018). Soluble tau aggregates, not large fibrils, are the toxic species that display seeding and cross-seeding behavior. *Protein Science*, *27*(11), 1901–1909. https://doi.org/10.1002/pro.3499

Glick, D., Barth, S., & Macleod, K. F. (2010). Autophagy: Cellular and molecular mechanisms. *The Journal of Pathology*, *221*(1), 3–12. https://doi.org/10.1002/path.2697

Groll, M., & Huber, R. (2003). Substrate access and processing by the 20S proteasome core particle. *The International Journal of Biochemistry & Cell Biology*, *35*(5), 606–616. https://doi.org/10.1016/S1357-2725(02)00390-4

Hicke, L. (2001). Protein regulation by monoubiquitin. *Nature Reviews Molecular Cell Biology*, *2*(3), 195–201. https://doi.org/10.1038/35056583

Jinwal, U. K., Akoury, E., Abisambra, J. F., O'Leary, J. C., Thompson, A. D., Blair, L. J., Jin, Y., Bacon, J., Nordhues, B. A., Cockman, M., Zhang, J., Li, P., Zhang, B., Borysov, S., Uversky, V. N., Biernat, J., Mandelkow, E., Gestwicki, J. E., Zweckstetter, M., & Dickey, C. A. (2013). Imbalance of Hsp70 family variants fosters tau accumulation. *The FASEB Journal*, *27*(4), 1450–1459. https://doi.org/10.1096/fj.12-220889

Kocaturk, N. M., & Gozuacik, D. (2018). Crosstalk Between Mammalian Autophagy and the Ubiquitin-Proteasome System. *Frontiers in Cell and Developmental Biology*, *6*, 128. https://doi.org/10.3389/fcell.2018.00128

Komander, D., & Rape, M. (2012). The Ubiquitin Code. *Annual Review of Biochemistry*, *81*(1), 203–229. https://doi.org/10.1146/annurev-biochem-060310-170328

Krüger, U., Wang, Y., Kumar, S., & Mandelkow, E.-M. (2012). Autophagic degradation of tau in primary neurons and its enhancement by trehalose. *Neurobiology of Aging*, *33*(10), 2291–2305. https://doi.org/10.1016/j.neurobiolaging.2011.11.009

Lamark, T., Perander, M., Outzen, H., Kristiansen, K., Øvervatn, A., Michaelsen, E., Bjørkøy, G., & Johansen, T. (2003). Interaction Codes within the Family of Mammalian Phox and Bem1p Domain-containing Proteins. *Journal of Biological Chemistry*, *278*(36), 34568–34581. https://doi.org/10.1074/jbc.M303221200

Lee, M. J., Lee, J. H., & Rubinsztein, D. C. (2013). Tau degradation: The ubiquitin–proteasome system versus the autophagy-lysosome system. *Progress in Neurobiology*, *105*, 49–59. https://doi.org/10.1016/j.pneurobio.2013.03.001

Li, L., Jiang, Y., Wang, J.-Z., Liu, R., & Wang, X. (2022). Tau Ubiquitination in Alzheimer's Disease. *Frontiers in Neurology*, *12*, 786353. https://doi.org/10.3389/fneur.2021.786353

Li, X., Huang, M., Zheng, H., Wang, Y., Ren, F., Shang, Y., Zhai, Y., Irwin, D. M., Shi, Y., Chen, D., & Chang, Z. (2008). CHIP promotes Runx2 degradation and negatively regulates osteoblast differentiation. *The Journal of Cell Biology*, *181*(6), 959–972. https://doi.org/10.1083/jcb.200711044

Long, J. M., & Holtzman, D. M. (2019). Alzheimer Disease: An Update on Pathobiology and Treatment Strategies. *Cell*, *179*(2), 312–339. https://doi.org/10.1016/j.cell.2019.09.001

Lutz, J., Höllmüller, E., Scheffner, M., Marx, A., & Stengel, F. (2020). The Length of a Ubiquitin Chain: A General Factor for Selective Recognition by Ubiquitin-

Binding Proteins. *Angewandte Chemie International Edition*, *59*(30), 12371–12375. https://doi.org/10.1002/anie.202003058

Maspero, E., & Polo, S. (2016). In Vitro Ubiquitination: Self-Ubiquitination, Chain Formation, and Substrate Ubiquitination Assays. In R. Matthiesen (Hrsg.), *Proteostasis* (Bd. 1449, S. 153–160). Springer New York. https://doi.org/10.1007/978-1-4939-3756-1_7

McDonough, H., & Patterson, C. (2003). CHIP: A link between the chaperone and proteasome systems. *Cell Stress & Chaperones*, *8*(4), 303. https://doi.org/10.1379/1466-1268(2003)008<0303:CALBTC>2.0.CO;2

Medeiros, R., Baglietto-Vargas, D., & LaFerla, F. M. (2011). The Role of Tau in Alzheimer's Disease and Related Disorders. *CNS Neuroscience & Therapeutics*, *17*(5), 514–524. https://doi.org/10.1111/j.1755-5949.2010.00177.x

Morishima-Kawashima, M., Hasegawa, M., Takio, K., Suzuki, M., Titani, K., & Ihara, Y. (1993). Ubiquitin is conjugated with amino-terminally processed tau in paired helical filaments. *Neuron*, *10*(6), 1151–1160. https://doi.org/10.1016/0896-6273(93)90063-W

Mukhopadhyay, D., & Riezman, H. (2007). Proteasome-Independent Functions of Ubiquitin in Endocytosis and Signaling. *Science*, *315*(5809), 201–205. https://doi.org/10.1126/science.1127085

Munari, F., Mollica, L., Valente, C., Parolini, F., Kachoie, E. A., Arrigoni, G., D'Onofrio, M., Capaldi, S., & Assfalg, M. (2022). Structural Basis for Chaperone-Independent Ubiquitination of Tau Protein by Its E3 Ligase CHIP. *Angewandte Chemie International Edition*, *61*(15), e202112374. https://doi.org/10.1002/anie.202112374

Nadel, C. M., Thwin, A. C., Callahan, M., Lee, K., Connelly, E., Craik, C. S., Southworth, D. R., & Gestwicki, J. E. (2023). The E3 Ubiquitin Ligase, CHIP/STUB1, Inhibits Aggregation of Phosphorylated Proteoforms of Microtubule-associated Protein Tau (MAPT). *Journal of Molecular Biology*, *435*(11),

168026. https://doi.org/10.1016/j.jmb.2023.168026

Nguyen, H. C., Wang, W., & Xiong, Y. (2017). Cullin-RING E3 Ubiquitin Ligases: Bridges to Destruction. In J. R. Harris & J. Marles-Wright (Eds.), *Macromolecular Protein Complexes* (Vol. 83, pp. 323–347). Springer International Publishing. https://doi.org/10.1007/978-3-319-46503-6_12

Ohi, M. D., Vander Kooi, C. W., Rosenberg, J. A., Chazin, W. J., & Gould, K. L. (2003). Structural insights into the U-box, a domain associated with multi-ubiquitination. *Nature Structural & Molecular Biology*, *10*(4), 250–255. https://doi.org/10.1038/nsb906

Petrucelli, L. (2004). CHIP and Hsp70 regulate tau ubiquitination, degradation and aggregation. *Human Molecular Genetics*, *13*(7), 703–714. https://doi.org/10.1093/hmg/ddh083

Puangmalai, N., Sengupta, U., Bhatt, N., Gaikwad, S., Montalbano, M., Bhuyan, A., Garcia, S., McAllen, S., Sonawane, M., Jerez, C., Zhao, Y., & Kayed, R. (2022). Lysine 63-linked ubiquitination of tau oligomers contributes to the pathogenesis of Alzheimer's disease. *Journal of Biological Chemistry*, *298*(4), 101766. https://doi.org/10.1016/j.jbc.2022.101766

Qiu, Y. (2021). *Tau ubiquitination and condensate formation with autophagy cargo receptors p62 and NBR1*. https://doi.org/10.25365/THESIS.70499

Quintana-Gallardo, L., Martín-Benito, J., Marcilla, M., Espadas, G., Sabidó, E., & Valpuesta, J. M. (2019). The cochaperone CHIP marks Hsp70- and Hsp90-bound substrates for degradation through a very flexible mechanism. *Scientific Reports*, *9*(1), 5102. https://doi.org/10.1038/s41598-019-41060-0

Richard, T. J. C., Herzog, L. K., Vornberger, J., Rahmanto, A. S., Sangfelt, O., Salomons, F. A., & Dantuma, N. P. (2020). K63-linked ubiquitylation induces global sequestration of mitochondria. *Scientific Reports*, *10*(1), 22334. https://doi.org/10.1038/s41598-020-78845-7

Rosenzweig, R., Nillegoda, N. B., Mayer, M. P., & Bukau, B. (2019). The Hsp70

chaperone network. *Nature Reviews Molecular Cell Biology*, *20*(11), 665–680. https://doi.org/10.1038/s41580-019-0133-3

Sarkar, M., Kuret, J., & Lee, G. (2008). Two motifs within the tau microtubule-binding domain mediate its association with the hsc70 molecular chaperone. *Journal of Neuroscience Research*, *86*(12), 2763–2773. https://doi.org/10.1002/jnr.21721

Scheufler, C., Brinker, A., Bourenkov, G., Pegoraro, S., Moroder, L., Bartunik, H., Hartl, F. U., & Moarefi, I. (2000). Structure of TPR Domain–Peptide Complexes. *Cell*, *101*(2), 199–210. https://doi.org/10.1016/S0092-8674(00)80830-2

Shibata, Y., & Komander, D. (2022). LUBAC. Current Biology, 32(11), R506–R508. https://doi.org/10.1016/j.cub.2022.04.041

Shimura, H., Schwartz, D., Gygi, S. P., & Kosik, K. S. (2004). CHIP-Hsc70 Complex Ubiquitinates Phosphorylated Tau and Enhances Cell Survival. *Journal of Biological Chemistry*, *279*(6), 4869–4876. https://doi.org/10.1074/jbc.M305838200

Shukla, D., & Trout, B. L. (2011). Understanding the Synergistic Effect of Arginine and Glutamic Acid Mixtures on Protein Solubility. *The Journal of Physical Chemistry B*, *115*(41), 11831–11839. https://doi.org/10.1021/jp204462t

Singh, S. K., Sahu, I., Mali, S. M., Hemantha, H. P., Kleifeld, O., Glickman, M. H., & Brik, A. (2016). Synthetic Uncleavable Ubiquitinated Proteins Dissect Proteasome Deubiquitination and Degradation, and Highlight Distinctive Fate of Tetraubiquitin. *Journal of the American Chemical Society*, *138*(49), 16004–16015. https://doi.org/10.1021/jacs.6b09611

Smith, M. C., Scaglione, K. M., Assimon, V. A., Patury, S., Thompson, A. D., Dickey, C. A., Southworth, D. R., Paulson, H. L., Gestwicki, J. E., & Zuiderweg, E. R. P. (2013). The E3 Ubiquitin Ligase CHIP and the Molecular Chaperone Hsc70 Form a Dynamic, Tethered Complex. *Biochemistry*, *52*(32), 5354–5364. https://doi.org/10.1021/bi4009209

Sun, M., & Zhang, X. (2022). Current methodologies in protein ubiquitination

characterization: From ubiquitinated protein to ubiquitin chain architecture. *Cell & Bioscience*, *12*(1), 126. https://doi.org/10.1186/s13578-022-00870-y

Tan, J. M. M., Wong, E. S. P., Kirkpatrick, D. S., Pletnikova, O., Ko, H. S., Tay, S.-P., Ho, M. W. L., Troncoso, J., Gygi, S. P., Lee, M. K., Dawson, V. L., Dawson, T. M., & Lim, K.-L. (2008). Lysine 63-linked ubiquitination promotes the formation and autophagic clearance of protein inclusions associated with neurodegenerative diseases. *Human Molecular Genetics*, *17*(3), 431–439. https://doi.org/10.1093/hmg/ddm320

Tanaka, K. (2009). The proteasome: Overview of structure and functions. *Proceedings of the Japan Academy, Series B*, *85*(1), 12–36. https://doi.org/10.2183/pjab.85.12

Thrower, J. S. (2000). Recognition of the polyubiquitin proteolytic signal. *The EMBO Journal*, *19*(1), 94–102. https://doi.org/10.1093/emboj/19.1.94

Tsuchiya, H., Burana, D., Ohtake, F., Arai, N., Kaiho, A., Komada, M., Tanaka, K., & Saeki, Y. (2018). Ub-ProT reveals global length and composition of protein ubiquitylation in cells. *Nature Communications*, *9*(1), 524. https://doi.org/10.1038/s41467-018-02869-x

Turco, E., Savova, A., Gere, F., Ferrari, L., Romanov, J., Schuschnig, M., & Martens, S. (2021). Reconstitution defines the roles of p62, NBR1 and TAX1BP1 in ubiquitin condensate formation and autophagy initiation. *Nature Communications*, *12*(1), 5212. https://doi.org/10.1038/s41467-021-25572-w

Walden, H., & Rittinger, K. (2018). RBR ligase–mediated ubiquitin transfer: A tale with many twists and turns. *Nature Structural & Molecular Biology*, *25*(6), 440–445. https://doi.org/10.1038/s41594-018-0063-3

Walinda, E., Morimoto, D., Sugase, K., Konuma, T., Tochio, H., & Shirakawa, M. (2014). Solution Structure of the Ubiquitin-associated (UBA) Domain of Human Autophagy Receptor NBR1 and Its Interaction with Ubiquitin and Polyubiquitin. *Journal of Biological Chemistry*, *289*(20), 13890–13902. https://doi.org/10.1074/jbc.M114.555441

Wang, G., Chen, X., Yu, C., Shi, X., Lan, W., Gao, C., Yang, J., Dai, H., Zhang, X., Zhang, H., Zhao, B., Xie, Q., Yu, N., He, Z., Zhang, Y., & Wang, E. (2024). Release of a ubiquitin brake activates OsCERK1-triggered immunity in rice. *Nature*, *629*(8014), 1158–1164. https://doi.org/10.1038/s41586-024-07418-9

Wang, T., Wang, W., Wang, Q., Xie, R., Landay, A., & Chen, D. (2020). The E3 ubiquitin ligase CHIP in normal cell function and in disease conditions. *Annals of the New York Academy of Sciences*, *1460*(1), 3–10. https://doi.org/10.1111/nyas.14206

Wang, Y.-S., Wu, K.-P., Jiang, H.-K., Kurkute, P., & Chen, R.-H. (2020). Branched Ubiquitination: Detection Methods, Biological Functions and Chemical Synthesis. *Molecules*, *25*(21), 5200. https://doi.org/10.3390/molecules25215200

Wesseling, H., Mair, W., Kumar, M., Schlaffner, C. N., Tang, S., Beerepoot, P., Fatou, B., Guise, A. J., Cheng, L., Takeda, S., Muntel, J., Rotunno, M. S., Dujardin, S., Davies, P., Kosik, K. S., Miller, B. L., Berretta, S., Hedreen, J. C., Grinberg, L. T., … Steen, J. A. (2020). Tau PTM Profiles Identify Patient Heterogeneity and Stages of Alzheimer's Disease. *Cell*, *183*(6), 1699-1713.e13. https://doi.org/10.1016/j.cell.2020.10.029

Wu, K., DeVita, R. J., & Pan, Z.-Q. (2024). Monoubiquitination empowers ubiquitin chain elongation. *Journal of Biological Chemistry*, *300*(3), 105753. https://doi.org/10.1016/j.jbc.2024.105753

Wu, S.-J., Liu, F.-H., Hu, S.-M., & Wang, C. (2001). Different combinations of the heat-shock cognate protein 70 (hsc70) C-terminal functional groups are utilized to interact with distinct tetratricopeptide repeat-containing proteins. *Biochemical Journal*, *359*(2), 419–426. https://doi.org/10.1042/bj3590419

Wurzer, B., Zaffagnini, G., Fracchiolla, D., Turco, E., Abert, C., Romanov, J., & Martens, S. (2015). Oligomerization of p62 allows for selection of ubiquitinated cargo and isolation membrane during selective autophagy. *eLife*, *4*, e08941. https://doi.org/10.7554/eLife.08941

Yang, Q., Zhao, J., Chen, D., & Wang, Y. (2021). E3 ubiquitin ligases: Styles, structures and functions. *Molecular Biomedicine*, *2*(1), 23. https://doi.org/10.1186/s43556-021-00043-2

Ye, Y., & Rape, M. (2009). Building ubiquitin chains: E2 enzymes at work. *Nature Reviews Molecular Cell Biology*, *10*(11), 755–764. https://doi.org/10.1038/nrm2780

Zhang, H., Amick, J., Chakravarti, R., Santarriaga, S., Schlanger, S., McGlone, C., Dare, M., Nix, J. C., Scaglione, K. M., Stuehr, D. J., Misra, S., & Page, R. C. (2015). A Bipartite Interaction between Hsp70 and CHIP Regulates Ubiquitination of Chaperoned Client Proteins. *Structure*, *23*(3), 472–482. https://doi.org/10.1016/j.str.2015.01.003

Zheng, N., & Shabek, N. (2017). Ubiquitin Ligases: Structure, Function, and Regulation. *Annual Review of Biochemistry*, *86*(1), 129–157. https://doi.org/10.1146/annurev-biochem-060815-014922